Theory of partial thermoremanent magnetization in multidomain grains
1. Repeated identical barriers to wall motion (single microcoercivity)

David J. Dunlop and Song Xu

Geophysics Laboratory, Department of Physics, University of Toronto, Toronto, Canada

We extend the Néel (1955) theory of thermoremanent magnetization (TRM) in multidomain grains to include (1) the acquisition of partial TRM produced by cooling from T_2 to T_1 in an applied field $\mathbf{H}_o$ and (2) the thermal demagnetization of partial and total TRM. If T_2 is $\geq 1°C$ below the Curie temperature T_c, the internal demagnetizing field $-NM_s$ (M_s is saturation magnetization and N is demagnetizing factor) is larger than geophysically reasonable values of H_o. The initial state for partial TRM blocking is then close to a demagnetized state and is quite different from the near-saturation initial state modeled by Néel for TRM blocking. As a result, a partial TRM $M_{ptr}(T_2, T_1, H_o)$ usually has a considerably lower intensity than total TRM $M_{tr}(T_c, T_o, H_o)$ or partial TRM $M_{ptr}(T_c, T_1, H_o)$. However, during thermal demagnetization, M_{tr} or $M_{ptr}(T_c, T_1, H_o)$ will begin to disappear at lower temperatures than $M_{ptr}(T_2, T_1, H_o)$ and exactly the same stable remanence will be isolated at high temperatures in all three cases. Blocking and unblocking do not occur at the same temperature as in the case of single-domain grains: TRM or partial TRM blocking is a sharp process (apart from possible reequilibration of walls when $H_o \rightarrow 0$), but thermal unblocking proceeds gradually toward a demagnetized state by continuous wall reequilibration and is complete only close to T_c. Above a threshold temperature T_{crit}, which is dependent on the type of partial TRM, the remanence intensity decreases in proportion to $H_c(T)$ for continuous thermal demagnetization or $\propto H_c(T)/M_s(T)$ for stepwise thermal demagnetization, where H_c is average microcoercivity. Because a grain with a single microcoercivity can acquire partial TRMs in many different blocking temperature ranges, each with a different set of wall displacements, Thellier's Law of Additivity of partial TRMs is only very approximately obeyed and the various partial TRMs are not independent.

1. Introduction

Thermoremanent magnetization (TRM) carried by single-domain grains has a number of experimental properties that make it an ideal recorder of the direction and intensity of the ancient geomagnetic field. Chief among these are the following:

1. The vector TRM $\mathbf{M}_{tr}$ is parallel to the applied field $\mathbf{H}_o$ during cooling.
2. TRM intensity M_{tr} is proportional to H_o for small fields.
3. $\mathbf{M}_{tr}$ is a sum of independent and additive partial TRMs, $\mathbf{M}_{ptr}$.
4. High-temperature partial TRMs are resistant to AF or thermal demagnetization.
5. In particular, a partial TRM is thermally erased over exactly the same temperature interval in which it was originally acquired.

Most of these properties are explained in a satisfying way by the theory of *Néel* [1949], whose central concept is the blocking temperature T_B, a "sharp" temperature (in reality a narrow temperature interval) at which partial TRM is frozen in during cooling. The temperature at which partial TRM is lost during zero-field heating is the unblocking temperature T_{UB}. T_{UB} is also comparatively sharp and for small fields $T_{UB} = T_B$.

Paper number 93JB02566.
0148-0227/94/93JB-02566$05.00

The TRM and partial TRM of multidomain grains are more problematic. In large grains containing many domain walls, TRM acquisition and demagnetization result from two processes, domain wall pinning/unpinning and nucleation/denucleation of domains and walls ("transdomain TRM"). In either case, following a change involving any one of the walls, the internal demagnetizing field $\mathbf{H}_d$ will cause all the other walls to reequilibrate. Unpinning and nucleation/denucleation are observed to occur readily when magnetite or titanomagnetite are mildly heated [*Halgedahl*, 1987; *Metcalf and Fuller*, 1987; *Heider et al.*, 1988], and this has led to a general feeling that multidomain TRM is untrustworthy as a paleofield recorder.

There are two reasons for taking a hard look at this conclusion. First is the practical consideration that a great deal of the paleomagnetic record, continental and oceanic, comes from magnetite or titanomagnetite grains which are of pseudo-single-domain (PSD) size. A fraction of these grains fail to nucleate any walls and acquire single-domain TRM in some coolings but develop a wall or walls in other coolings, while other grains always nucleate walls [*Halgedahl*, 1991]. Although single-domain TRM will be the most stable part of PSD TRM, wall-controlled TRM cannot be ignored. Second, many studies show that thermal demagnetization of TRM in large magnetite and titanomagnetite grains is not sharp but continuous [*Parry*, 1979; *Bolshakov and Shcherbakova*, 1979; *Tucker and O'Reilly*, 1980; *Hartstra*, 1982, 1983; *Worm et al.*, 1988]. Even quite low-temperature partial TRMs have thermal demagnetization tails extending to the Curie temperature T_c. Although multi-

domain partial (and total) TRM is easy to AF demagnetize in the laboratory, part of it very effectively resists demagnetization by reheating. Thus during reheating in nature, for example during burial metamorphism, a fraction of multidomain partial TRM will survive.

The purpose of this paper (hereinafter referred to as paper 1) and its companion [*Xu and Dunlop*, this issue] (hereinafter referred to as paper 2) is to develop a quantitative theory of multidomain partial TRM and thermal demagnetization. These aspects were not examined in *Néel*'s [1955] theory of total TRM or in subsequent theories. Wall pinning/unpinning with a single microcoercivity H_c is the subject of paper 1. Paper 2 extends the theory to walls encountering a distribution of microcoercivities whose average is H_c and compares our predictions with experimental observations. Transdomain TRM will be the subject of a future paper (D.J. Dunlop, A.J. Newell and R.J. Enkin, manuscript in preparation, 1994).

2. DOMAIN WALL PINNING AND ISOTHERMAL HYSTERESIS

Any real crystal contains lattice defects that pin domain walls. We can represent the pinning effect by a fluctuating domain wall energy, E_w. Figure 1 illustrates how E_w in a two-domain grain might depend on the displacement x of the domain wall from its central demagnetized position A. Minima in E_w correspond to locations where the wall is anchored by defects. Energy barriers between minima must be overcome by either thermal fluctuations or by an external applied field $\mathbf{H}_o$ before the wall will undergo a Barkhausen jump to another minimum energy position. Ignoring thermal energy for the moment and assuming that $\mathbf{H}_o$ is parallel to one of the domain magnetizations $\mathbf{M}_s$, the net magnetization M of a cube of side $2a$ and wall area A $(=4a^2)$ is $M = (x/a)M_s = rM_s$, where M_s is the saturation magnetization per unit volume. Physically, the quantity r represents either the relative wall displacement x/a or the fractional magnetization M/M_s. The total energy (wall + field + demagnetizing energies) of the model grain is approximately

$$E(x) = E_w - 2\mu_o AM_s H_o x + \mu_o NAM_s^2 x^2/a + \text{const}$$

$$= E_w - 2\mu_o Aa(H_o M - \frac{1}{2}NM^2) + \text{const}, \qquad (1)$$

where μ_o is the free-air magnetic permeability. In (1) we assume that the number of domains in a grain is constant, and thus the demagnetizing energy is adequately specified by a single demagnetizing factor N [e.g., *Dunlop*, 1983]. For minimum E, $dE/dx = 0$, and so

$$\frac{dE_w}{dx} = 2\mu_o AM_s(H_o - NM) = 2\mu_o AM_s H_i, \qquad (2)$$

$\mathbf{H}_i = \mathbf{H}_o - \mathbf{H}_d = \mathbf{H}_o - N\mathbf{M}$ being the average internal field.

The internal field required to displace the wall to pass an E_w maximum, like B in Figure 1, is the microscopic coercive force h_c, which can be defined as [e.g., *Xu and Merrill*, 1989]

$$h_c = \frac{1}{2\mu_o AM_s}\left|\frac{dE_w}{dx}\right|_{\max}. \qquad (3)$$

Externally, when a field

$$H_o = h_c + NM \qquad (4)$$

is applied to the grain, where M and h_c are measured at the point D where dE_w/dx is maximum, the wall is unpinned and makes a spontaneous jump from the point D to a point of steeper slope E in the neighboring E_w minimum. The jump is irreversible: the wall will not return to the original E_w minimum unless $\mathbf{H}_o$ is applied in the opposite direction. The negative critical field required to move the wall back from C to A is given by

$$H_o = -h_c + NM, \qquad (5)$$

in which h_c and M at the point of maximum negative slope F have been substituted in (5). Notice that this critical field is now numerically less than h_c. In general, $\mathbf{H}_o$ acts as the driving field for the wall, the demagnetizing field $\mathbf{H}_d$ acts as a restoring field assisting the wall towards a state of lower magnetization, and h_c acts as a resistive field impeding wall displacements in either direction.

Thus far we have described a minor loop in the hysteresis cycle. We assume below that E_w is periodic and symmetric, i.e. that the barriers to wall motion are regularly spaced and identical. This results in a rectangular major M–H_i loop with a single value of microcoercivity h_c equal to the measured bulk coercive force H_c for increasing or decreasing fields (Figure 2). The single wall

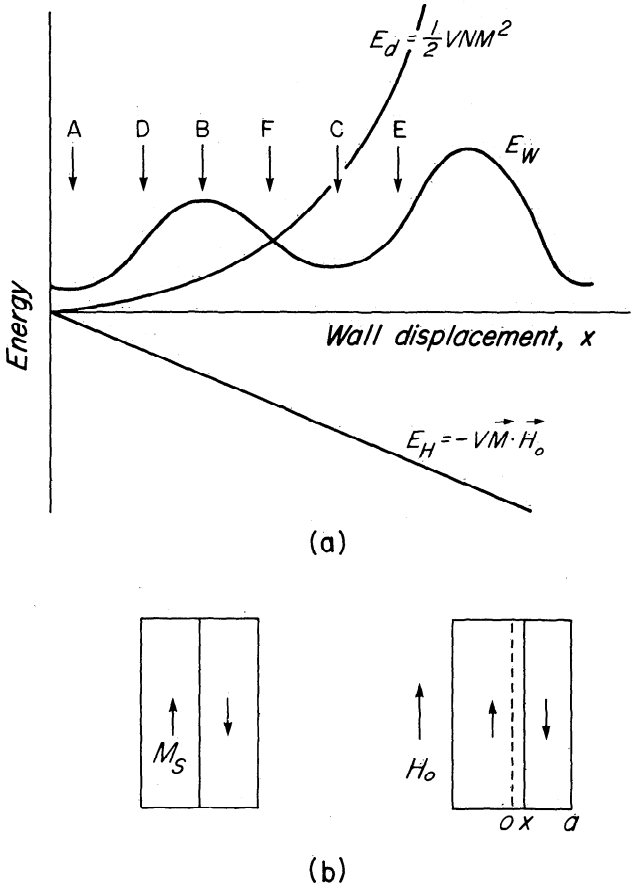

Fig. 1. Demagnetizing, wall and field energies E_d, E_w, and E_H as a function of the wall displacement x (in (a)) in a model grain (in (b)) of rectangular cross-section. Multiple walls with symmetric displacements can also be modeled. Because wall area is constant, the fractional wall displacement $r = x/a$ is equal to the fractional net magnetization M/M_s. For small $\mathbf{H}_o$, the wall(s) are pinned or confined to energy wells near local energy minimum positions (A and C for E_w; slightly different locations within the same wells for the total energy E). B marks a maximum in the wall energy, representing a barrier to wall displacement from A to C or vice versa. As H_o increases, the wall(s) displace to the right toward points of maximum slope in E_w (D, E). If $\mathbf{H}_o$ is reversed and increases in magnitude, a wall near C will be driven left toward a point of maximum negative slope (F).

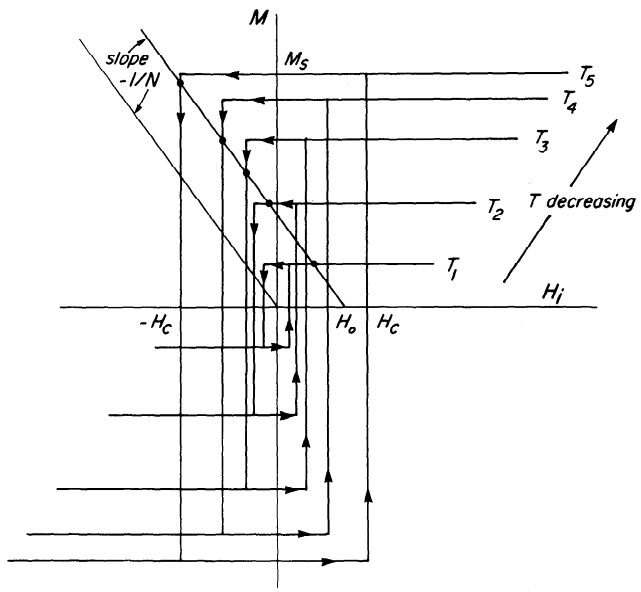

Fig. 2. Illustration of the process of field blocking of TRM. The magnetization M for an external field H_o at a given temperature T is given by the intersection (indicated by a dot) of the major loop with a line of intercept H_o and slope $-1/N$ (i.e., the graphical solution of (6)). At $T = T_1$ and T_2, the intersections give $M(T) = M_s(T)$ and thus the wall(s) is at its limiting position. In cooling below T_2, M at first descends the major loop, then (between T_4 and T_5) attempts to ascend the loop. At this point, the wall(s) has reversed its displacement and become field blocked at a local energy minimum like A or C in Figure 1. The intersection point for T_5 is therefore virtual; M/M_s cannot increase beyond the value it had at T_B ($\approx T_4$).

considered at the outset can be generalized to a series of walls which undergo symmetric displacements. In paper 2 [*Xu and Dunlop*, this issue] we will consider the effect of a distribution of microcoercivities.

Following *Néel* [1955], the externally measured $(M-H_o)$ hysteresis loop can be obtained by solving the two parametric equations

$$M = f(H_i), \tag{6a}$$

that is, $H_i = \pm H_c$ (rectangular loop)

$$M = \frac{H_o - H_i}{N}, \tag{6b}$$

that is, $H_i = H_o - NM$.

The first equation describes the internal field hysteresis loop whose ascending and descending branches are specified by $H_i = \pm H_c$ for a rectangular loop and the second equation relates internal and external fields. Solving these equations, we find that the external field hysteresis loop is given by

$$M = \frac{H_o \pm H_c}{N}. \tag{7}$$

The measured loop is "sheared"; the ascending and descending branches have slopes $1/N$.

Néel [1955] took a similar approach to multidomain TRM, first modeling the magnetization process using $M-H_i$ loops and then solving for the external field results using (6). We shall follow and extend this approach. *Schmidt* [1973] took the direct approach, beginning with the equivalent of (1) and showed that it gives results for TRM acquisition that are equivalent to Néel's.

3. BLOCKING OF TOTAL TRM

3.1. *The Field Blocking Process and the Blocking Temperature T_B*

TRM is acquired by cooling a grain in a constant field $\mathbf{H}_o$ from the Curie point T_c to room temperature T_o. At high temperatures, domain walls are less strongly pinned by defects. Empirically,

$$H_c(T) = H_{co}\left[\frac{M_s(T)}{M_{so}}\right]^n \equiv H_{co}\beta^n(T), \tag{8}$$

in which subscript o indicates room temperature value. Experimentally, values of n of 2-3 are often found [e.g., *Heider et al.*, 1987]. *Néel* [1955] assumed $n = 2$, while *Everitt* [1962], *Schmidt* [1973], and *Dunlop and Waddington* [1975] examined the effect of varying n. The essential point is that $n > 1$, so that H_c drops off more rapidly than H_d when the grain is heated above T_o. Comparing the three "fields" that control domain wall equilibrium, H_o is temperature independent, $H_d = -NM = -rNM_s(T) \propto \beta(T)$ for r fixed, and $H_c \propto \beta^n(T)$.

Immediately below T_c, H_d and H_c are both $\ll H_o$. Even a small applied field will drive the wall(s) to the grain boundary and saturate M. This is the situation depicted in Figure 2 at $T = T_1$ and T_2.

In cooling below T_2, $M_s(T)$ and thus $H_d(T)$ at first increase more rapidly, in percentage terms, than $H_c(T)$. When H_d becomes $> H_o$, the wall begins to be driven back from the boundary in a continuous reequilibration. Graphically, the intersection point moves down the descending branch of the major loop. The fractional wall displacement or magnetization $r = x/a = M/M_s$ decreases.

However, below T_4, $H_c(T)$ increases more rapidly than $H_d(T)$. The resistance to wall motion begins to outweigh the restoring force of self-demagnetization. The wall is held at a point of negative gradient $(dE_w/dx)_{\max}$, such as F in Figure 1, and cannot reverse its motion except locally in the E_w minimum centred on C. It cannot pass point E, without an increase in H_o. Graphically, the intersection point cannot ascend the descending branch of the major loop so as to increase the value of r. At this temperature T_B, where r reaches a minimum value $r_{\min}$ and the wall is trapped in a local E_w well, field blocking has occurred.

To find T_B explicitly, we solve (6) using for $f(H_i)$ the equation of the descending major loop, $H_i = -H_c(T)$, and have

$$M(T) = \frac{H_o + H_c(T)}{N} \tag{9a}$$

or

$$r(T) = \frac{x(T)}{a} = \frac{M(T)}{M_s(T)} = \frac{H_o + H_{co}\beta^n(T)}{NM_{so}\beta(T)}. \tag{9b}$$

Blocking (confinement to a local E_w minimum) occurs when $dr/dT = 0$, giving as the equation for T_B

$$H_c(T_B) = \frac{H_o}{n-1} \quad or \quad \beta(T_B) = \left[\frac{H_o}{(n-1)H_{co}}\right]^{1/n}. \tag{10}$$

We will refer to this situation as field blocking. In Figure 3, the values $H_{co} = 2$ mT (20 Oe), a value appropriate for multidomain magnetites, $H_o = 0.5$ mT (5 Oe), $n = 2$, $M_{so} = 480$ kA/m, and $N = 1/3$ ($4\pi/3$ in cgs) have been selected to illustrate how r changes during cooling from 575° to 295°C. The graphical solution consists of solving for the intersection of the descending major loop at each T,

$$H_i = -H_c(T), \tag{11a}$$

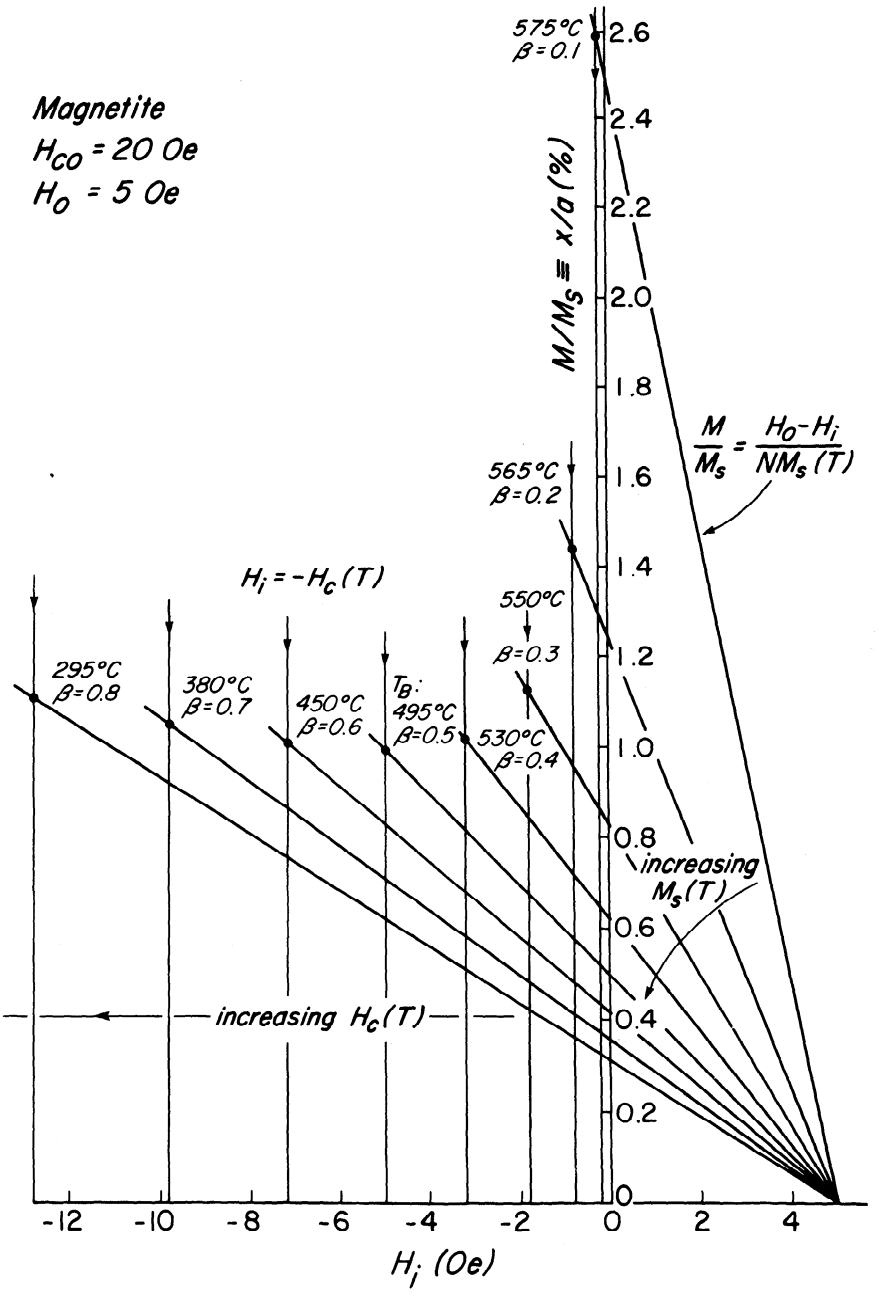

Fig. 3. A sample calculation of intersection points representing $r = M/M_s = x/a$ in the course of cooling magnetite grains from 575° to 295°C, using the method of Figure 2. The inclined lines model the increase in demagnetizing field $H_d = -NM$, driving the wall(s) back toward a demagnetized state, while the vertical lines represent the growth of microcoercivity H_c opposing wall motion. When H_c begins to outweigh H_d, r reaches a minimum value r_{min}, and wall motion is blocked (walls are trapped in local energy minima). This occurs at the blocking temperature T_B, which in this example is 495°C. (Note: 1 Oe = 0.1 mT.)

where $H_c(T)$ is given by (8), with

$$r = \frac{M}{M_s} = \frac{H_o - H_i}{NM_s(T)} \qquad (11b)$$

the relation between internal and external fields. Notice that the ordinate is $r = M/M_s$, not M as in (6*b*) and Figure 2. The H_o–H_i relation (11*b*) now plots as a different line at each temperature, but the advantage is that r_{min}, that is, blocking, is obvious. In this example, $T_B = 495°C$ ($\beta = 0.5$), at which point $H_c(T)$ has increased to $\beta^2 H_{co} = 0.5$ mT $= H_o$, as predicted by (10).

Figure 4 traces the succession of r values during cooling when $H_{co} = 2$ mT and $n = 2$ for applied fields of 0.05, 0.1, 0.2, 0.5, 1, and 1.5 mT. In each case, the r values beyond r_{min} have no physical reality; this virtual part of the r curve is shown dashed. For each H_o, blocking occurs when $H_c(T)$ increases to a value equal to H_o, as seen from the corresponding blocking point on the $H_c(T)$ curve and expected from (10) when $n = 2$. Notice that blocking temperatures are always ≥500°C if $H_o < 0.5$ mT. For geomagnetically reasonable fields ≤ 0.1 mT, T_B is very high: 560°–570°C.

The dependence of T_B on applied field H_o and on microcoercivity H_{co}, for $n = 2$, is graphed in Figure 5 (see also *Schmidt* [1976] and *Dunlop* [1982]). For any reasonable choice of H_{co}, $T_B \geq 550°C$ for $H_o \leq 0.1$ mT. T_B values <495°C are not mean-

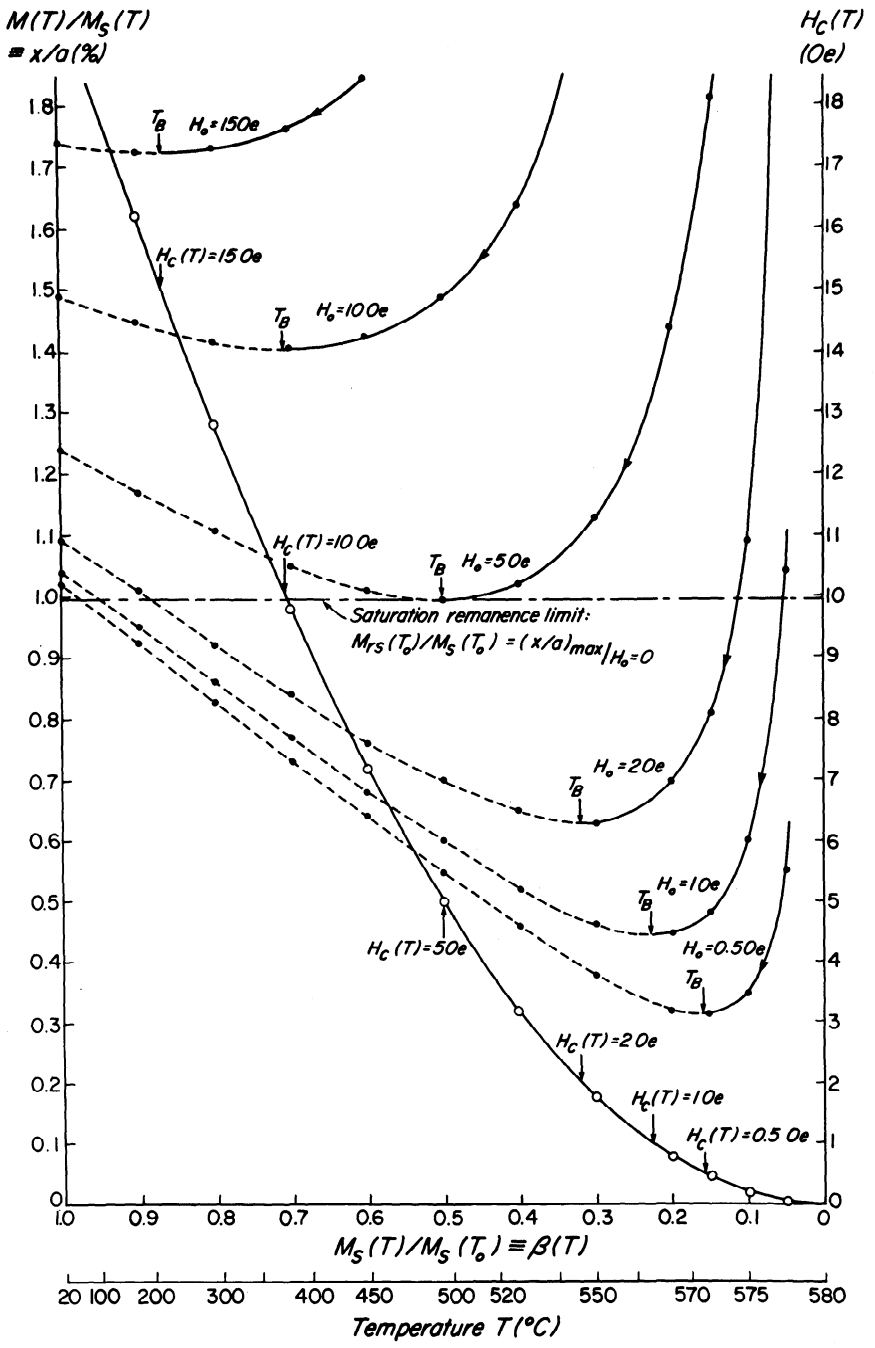

Fig. 4. The effect of field strength H_o on TRM blocking master curves (loci of M/M_s with decreasing T, calculated as in Figure 3; numerical values are indicated on the left-hand scale; dashed portions below T_B are unattainable because walls remain blocked at r_{min}). The blocking temperature T_B in each case satisfies the condition $H_c(T_B) = H_o$ (equation (10) with model parameters $H_{co} = 2$ mT, $n = 2$), as indicated by the alignment of the arrows marking T_B on each master curve directly above the corresponding values $H_c = H_o$ on the $H_c(T)$ curve (solid curve with open points and right-hand scale). T_B increases as H_o decreases. Above the line marked "saturation remanence limit," $M/M_s > M_{rs}/M_s$ at T_o, and the wall(s) reequilibrate when $H_o \to 0$ at T_o. (Note: 1 Oe = 0.1 mT.)

ingful for this value of n because the wall(s) become unblocked and reequilibrate below T_B when $H_o \to 0$. This situation, labeled "saturation remanence limit" on Figures 4 and 5, will be considered in section 3.3.

Assuming the wall or walls remain blocked below T_B, even when $H_o \to 0$ at T_o, the intensity of TRM $M_{tr}(T_o)$ is equal to $r_{min}(T_B)M_{so}$ or $M(T_B)/\beta(T_B)$. From (9) and (10),

$$M(T_B) = \frac{n}{n-1}\frac{H_o}{N} \tag{12}$$

and so

$$M_{tr}(T_o) = \frac{nH_{co}^{1/n}H_o^{1-1/n}}{(n-1)^{1-1/n}N}. \tag{13}$$

This result, or its equivalent, was derived by *Néel* [1955], *Everitt* [1962], *Schmidt* [1973], *Dunlop and Waddington* [1975], and *Day* [1977]. The screening effect of soft or loosely pinned walls which unblock when $H_o \to 0$ is ignored in (13).

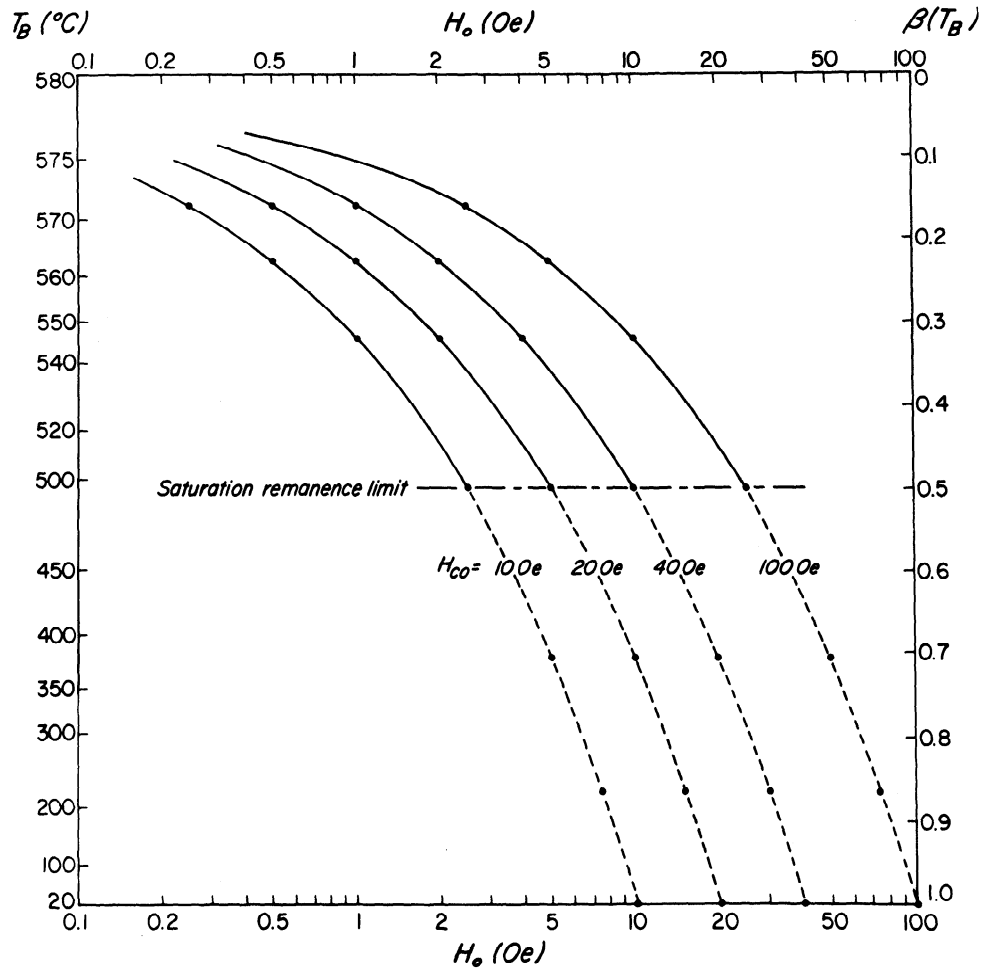

Fig. 5. The field dependence of TRM blocking temperature T_B for various values of H_{co} and $n = 2$, determined as in Figure 4 or directly from (10). (Note: 1 Oe = 0.1 mT.)

Notice that although $M(T_B) \propto H_o$, the room-temperature TRM intensity is not proportional to field strength, essentially because T_B is field dependent [cf. *Schmidt*, 1976]. (The exception is the limit $n \to \infty$, which yields the results of *Stacey* [1958, 1963] but is physically unrealistic, as discussed by *Dunlop and Waddington* [1975].) Since experimentally M_{tr} is $\propto H_o$ for fields of paleomagnetic interest, there must be a low-field limit below which (13) is no longer valid. There must also be a high-field limit, since M_{tr} cannot exceed the saturation remanence $M_{rs}(T_o)$. We now derive these limits.

3.2. *Low-Field Limit for Field-Blocked TRM*

When H_o is small, T_B approaches T_c (Figures 4 and 5). Then, as *Néel* [1955] pointed out, the blocking condition (10) no longer holds because $H_c(T_B)$, representing the pinning or resistance to wall motion, becomes so small that the wall can be unblocked by thermal fluctuations. That is, $H_c(T_B)$ is less than the thermal fluctuation field $H_f(T_B)$. Since H_c increases with cooling, whereas H_f decreases with cooling, we can define a new, lower blocking temperature T_{Bf} at which the pinning field equals the average fluctuation field:

$$H_c(T_{Bf}) = H_f(T_{Bf}) \quad \text{or} \quad \beta(T_{Bf}) = \left[\frac{H_f(T_{Bf})}{H_{co}}\right]^{1/n}. \tag{14}$$

The thermal fluctuation blocking temperature T_{Bf} is independent of applied field H_o.

The unpinned wall can move from one energy well to another on short timescales with the help of thermal energy, and the situation is analogous to thermal activation of single-domain moments. The most probable wall position is the one of minimum total energy E. Since we have assumed that all E_w minima are identical, the global minimum energy is determined by the balance between the self-demagnetizing and external field energies in (1), giving for the average magnetization at T_{Bf}

$$M(T_{Bf}) = \frac{H_o}{N}. \tag{15}$$

The room-temperature TRM is $M(T_{Bf})/\beta(T_{Bf})$. Combining (14) and (15), this gives

$$M_{tr}(T_o) = \frac{H_{co}^{1/n} H_o}{N H_f^{1/n}(T_{Bf})}. \tag{16}$$

We call this situation thermal blocking. Thermally blocked TRM is proportional to H_o, as observed experimentally for small fields.

The threshold field $(H_o)_f$ below which TRM is thermally blocked can be found by equating M_{tr} from (16) to M_{tr} for field blocking, as given by (13). This gives

$$(H_o)_f = \frac{n^n}{(n-1)^{n-1}} H_f(T_B). \tag{17}$$

When $n = 2$, $(H_o)_f = 4H_f(T_B)$, as reported by *Néel* [1955].

The fluctuation field H_f may be determined from

$$H_f(T) = \frac{kT\log(f_o t)}{2VM_s(T)}, \quad (18)$$

which assumes that thermal energy is transferred to domain walls via fluctuations in E_w barrier heights (cf. Figure 1) [*Street and Woolley*, 1949; *Néel*, 1955, p. 237; *Dunlop*, 1973, p. 878]. In (18), k is Boltzmann's constant, $f_o \approx 10^{-10}$ s is atomic reorganization time [*Gaunt*, 1977], t is experimental time, and V is the volume swept out by a domain wall in a Barkhausen jump. A theoretical estimate of H_f is usually difficult to make because the Barkhausen volume V required in (18) is unknown. Experimentally, $H_f(T_B)$ for multidomain grains is estimated from (17) to be ≈ 0.1 mT from the observed limit $(H_o)_f$ for linearity between TRM intensity and applied field strength.

3.3. *High-Field Limit for Field-Blocked TRM*

The high-field limit for field blocking occurs at a critical field $(H_o)_{crit}$ such that $M_{tr}(T_o)$ reaches the saturation remanence $M_{rs}(T_o)$. Cooling a grain in $H_o > (H_o)_{crit}$ will produce $M(T_o) > M_{rs}(T_o)$, but when $H_o \to 0$, the wall(s) will spring back to their saturation remanence position(s) under the restoring force of H_d. We will refer to this regime, in which the TRM blocked is equal to $M_{rs}(T_o)$ no matter what field is applied, as wall reequilibration.

To find $(H_o)_{crit}$ explicitly, we equate $M_{rs}(T_o)$, which is H_{co}/N according to (9*a*) (setting $H_o = 0$ and $T = T_o$), to the TRM intensity predicted by (13). The result is

$$(H_o)_{crit} = \frac{n-1}{n^{n/(n-1)}} H_{co} \quad (19)$$

so that the high-field breakpoint in TRM acquisition is proportional to H_{co}. $(H_o)_{crit}$ is not a large field: the factor $(n-1)/n^{n/(n-1)}$ is always < 1 (for $n = 2$, it is 0.25) and H_{co} for MD magnetite is typically ≤ 10 mT. In practice, the microcoercivity distribution is sufficiently broad that the changeover from field-blocked TRM to wall reequilibration TRM may be gradual rather than sharp.

Figure 6 compares some measured M_{tr}–H_o data with the predictions of (13), (16), and (19). The breakpoint $(H_o)_f$ between thermally blocked and field-blocked TRM has been arbitrarily set at 0.2 mT. The breakpoint $(H_o)_{crit}$ between field-blocked and wall reequilibration TRM was calculated assuming $H_{co} = 2$ or 5 mT, values appropriate for magnetite. Multidomain theory gives a better description of the data than single-domain theory, but the breakpoint fields are lower than those observed. Higher values for H_{co}, which may be justified for titanomagnetite, would raise $(H_o)_{crit}$ in the desired way but would also increase the saturation remanence intensity.

The limit for field blocking can also be expressed in terms of a minimum blocking temperature $(T_B)_{min}$. Predicted T_B values

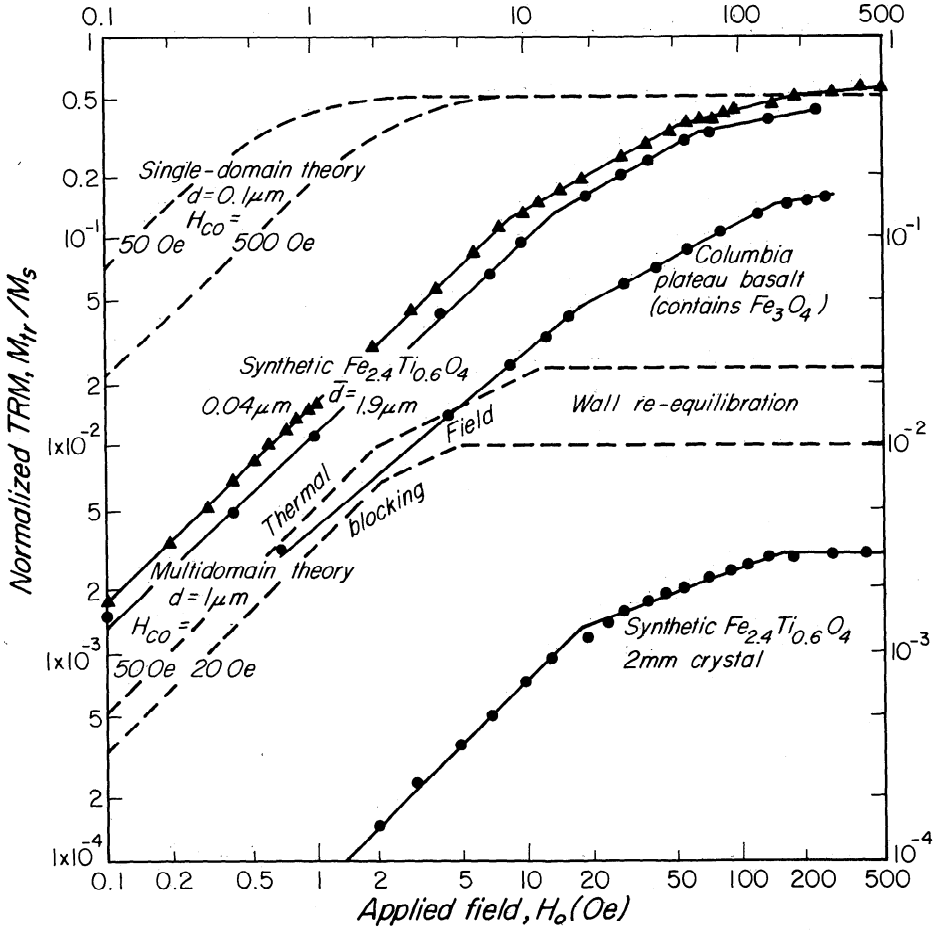

Fig. 6. The field dependence of TRM intensity, comparing data for multidomain samples from *Dunlop and Waddington* [1975] (Columbia plateau basalt), *Day* [1977] and *Tucker and O'Reilly* [1980] (synthetic $Fe_{2.4}Ti_{0.6}O_4$ with mean grain sizes of 1.9 μm and 2 mm, respectively), and for a single-domain sample (synthetic $Fe_{2.4}Ti_{0.6}O_4$ with a mean grain size of 0.04 μm) from *Özdemir and O'Reilly* [1982] with the predictions of single-domain and multidomain TRM theory. The multidomain theoretical curves are independent of grain size, except in the thermal blocking (low-field) range, where a grain size of 1 μm and a Barkhausen jump of 30 nm have been assumed. (Note: 1 Oe = 0.1 mT.)

$< (T_B)_{min}$ (e.g., those shown in Figure 4 for $H_o > 0.5$ mT) do not represent true blocking temperatures because the walls reequilibrate at T_o when $H_o \to 0$. To find $(T_B)_{min}$, we combine (10) and (19), giving

$$\beta[(T_B)_{min}] = n^{-1/(n-1)}. \tag{20}$$

Notice that the critical temperature, unlike the critical field, is independent of microcoercivity. For $n = 2$, $(T_B)_{min} = 495°C$ for magnetite, as indicated by the saturation remanence limits in Figures 4 and 5. For $n > 2$, $(T_B)_{min}$ decreases, reaching 400°C when $n \approx 5$. Field blocking at temperatures much lower than 400°C would require unreasonably large values of n.

To summarize, total TRM is thermally blocked and varies linearly with H_o (equations (16) and (17)) if H_o is small ($\lesssim 0.1$–0.2 mT). Blocking temperatures T_{Bf} are very close to T_c. For intermediate fields, TRM is field blocked at a T_B in the range 500°–570°C approximately (for $n = 2$) and varies nonlinearly (quadratically for $n = 2$) with H_o (equations (10) and (13)). For larger fields (which are as low as 0.5-2.5 mT for $H_{co} = 2$–10 mT when $n = 2$), walls are blocked during cooling at a temperature lower than 500°C, but the walls reequilibrate and the magnetization is reduced to $M_{rs}(T_o) = H_{co}/N$ when the field is removed at room temperature. The field blocking—wall reequilibration boundary is most conveniently expressed by the minimum true blocking temperature $(T_B)_{min}$ (equation (20)).

4. THERMAL DEMAGNETIZATION OF TOTAL TRM

4.1. *Partial TRM Acquired Between T_c and T_B*

As a preliminary, consider a partial TRM in which the grain is cooled from T_c to a blocking temperature T_B (as defined in (10)) in a field H_o, and from T_B to T_o in zero field, and assume that H_o is such that we are in the field blocking regime for total TRM. When $H_o \to 0$ at T_B, the wall or walls will reequilibrate to give

$$M_r(T_B) = \frac{H_c(T_B)}{N} = \frac{H_o}{(n-1)N}, \tag{21}$$

using (9*a*) and (10). Since $M(T_B) = [n/(n-1)](H_o/N)$ according to (12), we see that

$$M_r(T_B) = \frac{M(T_B)}{n} \quad \text{or} \quad r_o(T_B) = \frac{r_H(T_B)}{n} \tag{22}$$

where r_H and r_o are relative wall displacements x/a in field H_o and zero field, respectively. Since the same x/a values are preserved in cooling to room temperature, the partial TRM measured at T_o is only a fraction $1/n$ of the total TRM measured at T_o.

We now enquire at what lower temperature T'_B the wall(s) will just remain blocked when $H_o \to 0$. A partial TRM acquired between T_c and T'_B will have the same intensity as the total TRM. The condition on T'_B is that

$$r_o(T'_B) = r_H(T_B) = nr_o(T_B) \quad \text{or} \quad \beta(T'_B) = n^{1/(n-1)}\beta(T_B) \tag{23}$$

using (9*b*) and (22). Obviously, if T'_B goes below T_o, one has passed from the field blocking to the wall reequilibration mode of total TRM acquisition. Thus another method of specifying the boundary between these regimes is to set $T'_B = T_o$, $T_B = (T_B)_{min}$ in the second equation of (23). Since $\beta(T_o) = 1$, we then have $\beta[(T_B)_{min}] = n^{-1/(n-1)}$, as in (20).

We can readily verify that partial TRM acquired between T_c and T'_B has the same intensity as total TRM. Using (9*b*), (23), and (10) successively, the partial TRM measured at T_o is

$$M_{ptr}(T_c, T'_B, H_o) = r_o(T'_B)M_{so} = \frac{H_{co}\beta^{n-1}(T'_B)}{N}$$

$$= \frac{nH_{co}\beta^{n-1}(T_B)}{N} = \frac{nH_{co}^{1/n}H_o^{1-1/n}}{(n-1)^{1-1/n}N}, \tag{24}$$

which agrees with the total TRM intensity from (13). It is obvious from (24) that as $T'_B \to T_o$, the partial TRM approaches the limiting value $H_{co}/N = M_{rs}(T_o)$, that is, that one passes from the field blocking to the wall reequilibration regime, as asserted in the previous paragraph.

4.2. *Thermal Demagnetization*

Now we are ready to deal with thermal demagnetization. During zero-field heating from T_o, walls will first unblock, and TRM will begin to demagnetize, at T'_B. After heating to T_B and cooling to T_o, the TRM will retain $1/n$ of its initial intensity; this is the same fraction that remains if $H_o \to 0$ at T_B during initial cooling (cf. equation (22)). To totally erase the TRM, one would have to heat close to T_c because only at very high temperatures does the demagnetizing field H_d sufficiently outweigh the resistance to wall motion (represented by H_c) to restore the wall(s) to their completely demagnetized position(s). High-temperature "tails" extending essentially to the Curie point have been observed during thermal demagnetization of TRM and partial TRM in magnetite and titanomagnetite by *Bolshakov and Shcherbakova* [1979], *Parry* [1979], *Tucker and O'Reilly* [1980], *Hartstra* [1982, 1983] and *Worm et al.* [1988]. (In reality, demagnetization will be complete at T_{Bf}, which is close to T_c.)

Thermal demagnetization in the field-blocking regime is illustrated in Figure 7. For the parameters assumed ($H_o = 0.5$ mT, $H_{co} = 2$ mT, $n = 2$), $T_B = 495°C$ and $T'_B = 20°C$. The values of $r_o(T) = M_r(T)/M_s(T)$ for each heating temperature T are the intersections between $H_i = -H_c(T)$ and $r = M/M_s = -H_i/NM_s(T)$ (cf. equations (6a) and (6b)). Notice that after heating to $T_B = 495°C$, the remanence drops to $1/n = 1/2$ of its initial intensity, as predicted above.

Quantitatively, the fraction of TRM remaining after heating to T in a stepwise thermal demagnetization experiment is

$$\frac{M_{ro}(T)}{M_{tr}(T_o)} = \frac{r_o(T)}{r_o(T'_B)} = \frac{\beta^{n-1}(T)}{\beta^{n-1}(T'_B)} \qquad T \geq T'_B \tag{25}$$

using (9*b*). Here M_{ro} denotes remanence measured at T_o, after zero-field cooling from T. If instead, remanence is measured at T in the course of zero-field heating (continuous thermal demagnetization),

$$\frac{M_r(T)}{M_{tr}(T_o)} = \frac{\beta(T)M_{ro}(T)}{M_{tr}(T_o)} = \frac{\beta^n(T)}{\beta^{n-1}(T'_B)} \qquad T \geq T'_B \tag{26}$$

Note that according to (25) and (23), $M_{ro}(T_B)/M_{tr}(T_o) = 1/n$, as we concluded earlier.

For the example of Figure 7, where $n = 2$ and $T'_B = 20°C$, (25) and (26) predict that total TRM will demagnetize in proportion to $M_s(T)$ in stepwise cleaning (this is the situation illustrated in Figure 7) or in proportion to $M_s^2(T)$ in continuous heating. Figure 8 graphs the stepwise cleaning, plotting M/M_o (replacing $M_{ro}(T)/M_{tr}(T_o)$) as a function of T. For $H_o = 0.5$ mT, the TRM decays linearly in proportion to β, as predicted in Figure 7. If $H_o > 0.5$ mT, $T'_B < T_o$ and $M_{tr} = M_{rs}$, which has the same thermal decay as the 0.5-mT TRM. When $H_o < 0.5$ mT, $T'_B > T_o$. In this case, the TRM has no unblocking temperatures below T'_B but demagnetizes linearly with β above T'_B. Notice that both T'_B

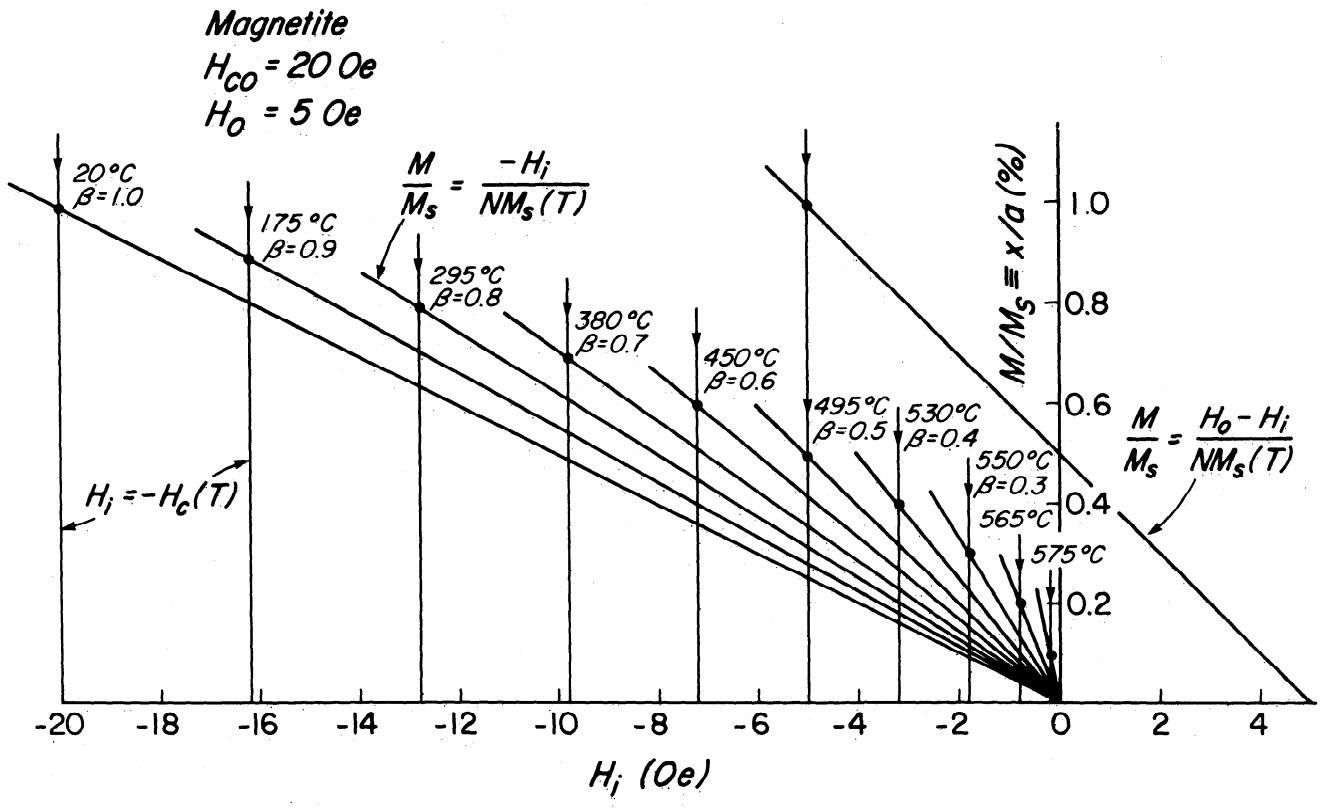

Fig. 7. Sample calculation of thermal demagnetization of TRM. TRM blocking with the same model parameters was shown in Figure 3. The blocking was sharp and occurred at T_B = 495°C, but unblocking is gradual and covers the entire range from T_o to T_c. The locus of intersection points between the zero-field demagnetizing characteristics (the lines of zero intercept and variable slope) and the descending major loops ($H_i = -H_c(T)$) defines the thermal demagnetization master curve, which goes as $r(T) \propto H_c(T)/M_s(T) \propto \beta^{n-1}(T)$. (Note: 1 Oe = 0.1 mT.)

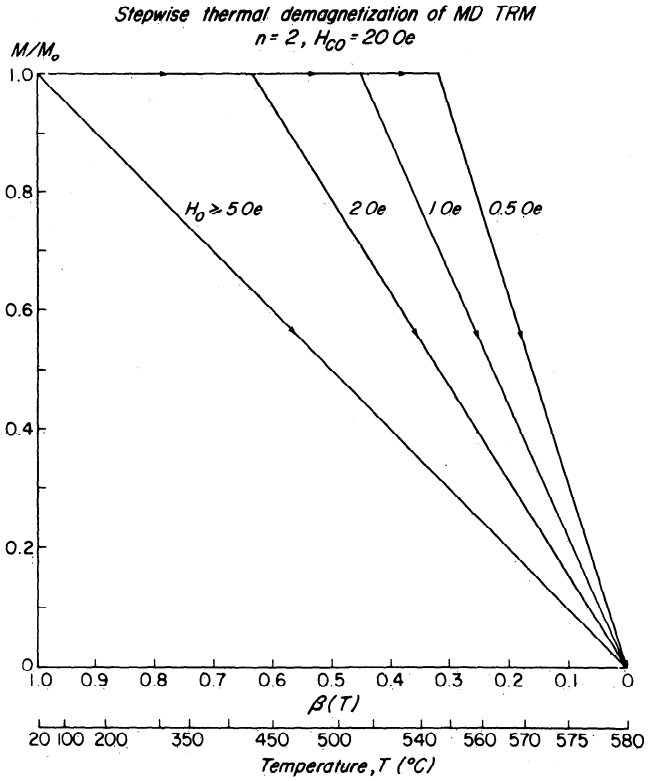

and T_B (the temperature at which $M/M_o = 1/n = 1/2$) increase as H_o decreases. The field dependence of T_B was illustrated in Figure 5; the field dependence of T'_B follows from (23).

5. Isothermal Remanence (IRM) at Temperature T

As a preliminary to modeling the blocking of partial TRM in the general case, we next consider the acquisition of an isothermal remanent magnetization in a field H_o at temperature T. We suppose walls to be initially in positions corresponding to a demagnetized state. If H_o is applied at T_c (580°C for magnetite), even a very small field will drive the walls to their limiting positions and produce a saturation magnetization. However, the saturation field $(H_o)_{sat} \approx H_c(T) + NM_s(T) \approx NM_s(T)$ increases rapidly with cooling. By T = 575°C, $(H_o)_{sat}$ is already ≈ 20 mT, so it is clear that at most temperatures, the major loop is inaccessible. Only minor loops will be traced out when H_o is applied and removed at temperature T to produce IRM.

Figure 9 illustrates a series of such minor loops. (The vertical heights of the minor loops have been exaggerated to bring the major loop on scale.) There are four possible cases.

Fig. 8. Simulated thermal demagnetization curves of TRM computed as in Figure 7. Above the minimum unblocking temperature T'_B, $r(T)$ follows the thermal demagnetization master curve $\propto \beta^{n-1}(T) = \beta(T)$ for n = 2. As H_o decreases, unblocking begins at higher and higher temperatures. (Note: 1 Oe = 0.1 mT.)

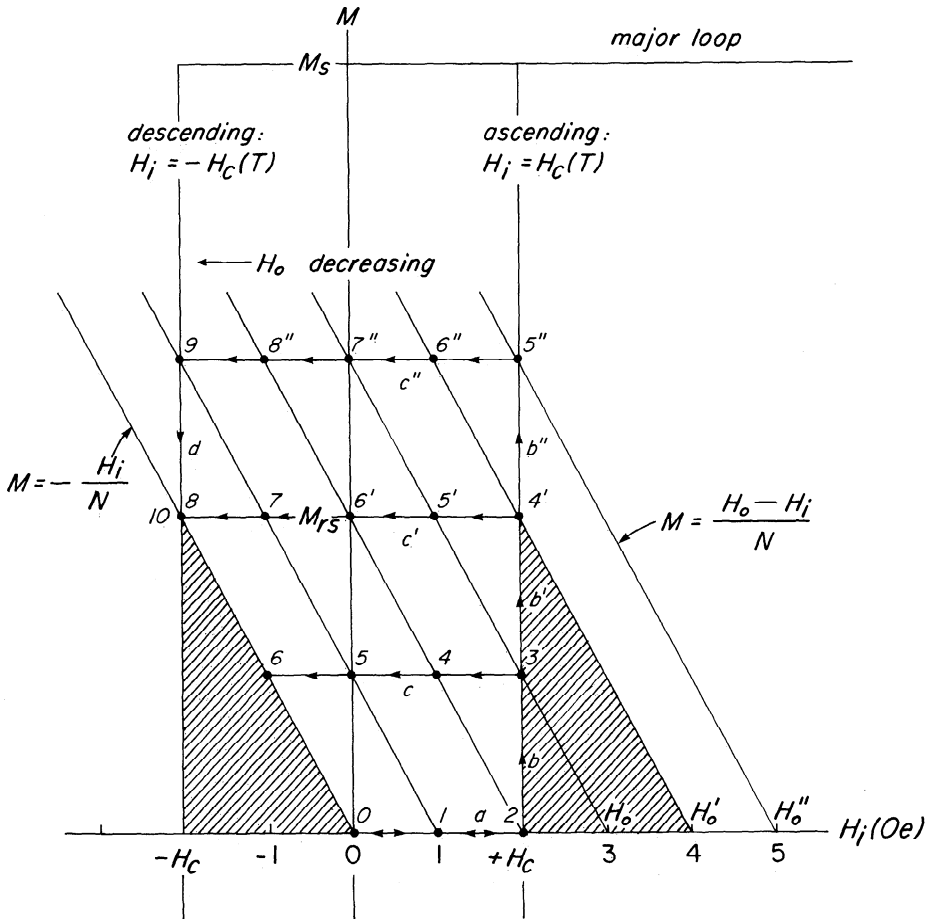

Fig. 9. Modeling acquisition of IRM at constant temperature T, starting from a demagnetized state. Four different cases are shown: (1) $H_o < H_c$ for which $M_r = 0$ (walls remain trapped); (2) $H_c \le H_o < 2H_c$ for which $M_r < M_{rs}(T)$ (walls unpinned and move to less than maximum displacements); (3) $H_o = 2H_c$ for which $M_r = M_{rs}(T)$ (walls pushed to maximum displacements); (4) $H_o > 2H_c$ for which $M_r = M_{rs}(T)$ (walls pushed beyond maximum zero-field displacements, but spring back to M_{rs} (reequilibrate) when $H_o \to 0$). (Note: 1 Oe = 0.1 mT.)

1. If $H_o < H_c(T)$, the wall(s) will not pass the nearest energy barrier(s) and path a will be followed (0-1-2-1-0). The IRM will be zero. For the parameters chosen in Figure 9, this situation of trapped walls occurs for $H_o < 0.2$ mT.

2. If $H_c(T) \le H_o < 2H_c(T)$, the wall(s) will pass one or more energy barriers. As H_o increases from zero, M will first follow path a, then will rise from zero along path b, following intersection points (e.g., point 3) of $M = (H_o - H_i)/N$ with the ascending major loop $H_i = H_c(T)$ (cf. equations (6a) and (6b)). When H_o begins to decrease, the walls cannot reverse their motion but remain trapped in local wells. On the M–H_i graph, points cannot descend the ascending major loop; they instead follow path c (e.g., points 3-4-5-6) of constant M, acquiring an IRM less than the saturation remanence $M_{rs}(T)$. In Figure 9 this is the situation if H_o is between 0.2 and 0.4 mT.

3. If $H_o = 2H_c(T)$, path a-b-b'-c' is followed (0-1-2-3-4′-5′-6′-7-8) on the M–H_i graph. Point 8, the intersection of $M(T) = -H_i/N$ with the descending major loop $H_i = -H_c(T)$, corresponds to the saturation remanence $M_{rs}(T) = H_c(T)/N$. Thus the walls have been driven further from the zero magnetization state, just reaching positions corresponding to saturation remanence. In Figure 9 this occurs if H_o reaches a maximum value $H_o' = 0.4$ mT.

4. If $H_o > 2H_c(T)$, walls will be driven past their saturation remanence positions as H_o increases to its maximum value (H_o''). M will follow the sequence 0-1-2-3-4′-5″. As H_o decreases from $H_o'' = 0.5$ mT to 0.1 mT, the walls remain trapped in local wells and M remains constant, following path c'' (5″-6″-7″-8″-9). Finally, as H_o decreases from 1 mT to zero, wall reequilibration occurs. The internal demagnetizing field drives walls past some barriers with negative slopes (cf. Figure 1) toward the demagnetized state, and the remanence drops to $M_{rs}(T)$ (path d: 9-10).

Case 2 will be labeled as "isothermal blocking", while case 4 corresponds to wall reequilibration as in TRM acquisition. The critical field H_o separating these two regimes is given by

$$H_o = 2H_c(T) \tag{27}$$

(i.e., case 3). This value of H_o is just sufficient to drive walls to the maximum displacements they can maintain in zero field at the same temperature T. Since the critical field is temperature dependent, the boundary between the regimes will shift as T decreases. This is the situation in the blocking of partial TRM, which we discuss next.

6. BLOCKING OF PARTIAL TRM

6.1. *Wall Reequilibration pTRM*

Since T changes in the course of pTRM acquisition, it is now advantageous to work with $M(T)/M_s(T)$, which is a direct measure of relative wall displacement $r = x/a$. Otherwise, the argument proceeds as in the last section. The sample is cooled from

T_c in zero field, from T_2 to T_1 in field H_o, and from T_1 to room temperature T_o in zero field. Figure 10 traces the process on an r–H_i graph for $H_o = 0.5$ mT, $T_2 = 550°C$ ($\beta = 0.3$) and various values of T_1 ($H_{co} = 2$ mT and $n = 2$ are assumed).

When H_o is applied at T_2, M/M_s follows path a-b to the intersection point labeled $T_2 = 550°C$. The induced magnetization is given explicitly by

$$\frac{M}{M_s} = \frac{H_o - H_c(T)}{NM_s(T)} \tag{28}$$

following the prescription given in (6) (cf. section 5, case 2). It amounts to about 0.53%. If H_o is removed at the same temperature T_2, we follow the path c-d to the intersection point labeled $T_1 = 550°C$, giving a normalized IRM of about 0.30%. If we cool to a lower temperature T_1, e.g., 530°C ($\beta = 0.4$), with H_o applied, a partial TRM will be acquired. Notice that the intersection point specified by (28) and labeled $T = 530°C$ in Figure 10 is only 0.225% and would require us to descend the ascending major loop. Since this is impossible, the walls are blocked at T_2 and remain trapped locally, in this case at $r = 0.53\%$, during field cooling to T_1.

When $H_o \to 0$ at T_1, the magnetization follows the path c-c'-d' to the intersection labeled $T_1 = 530°C$. Notice that the walls reequilibrate as the field decreases but not as much as they did at 550°C. The remanence, which is the saturation remanence at 530°C, remains blocked in zero-field cooling to T_o. The normalized partial TRM amounts to about 0.40%.

This is exactly 40% of the normalized total TRM produced by cooling in 0.5 mT from T_c to T_o, which was equal to the room-temperature saturation remanence and was very close to 1.0% (cf. Figures 3 and 4). Thus if wall reequilibration occurs in both partial and total TRM processes, the pTRM/TRM ratio is just the ratio of normalized saturation remanences at T_1 and T_o, independent of T_2. That is,

$$\frac{M_{ptr}(T_o)}{M_{tr}(T_o)} = \frac{r_o(T_1)}{r_o(T_o)} = \beta^{n-1}(T_1) \tag{29}$$

using equation (9b). It is obvious in Figure 10 that the three wall reequilibration pTRMs, acquired between $T_2 = 550°C$ and $T_1 = 550°C$ ($\beta = 0.3$), 530°C ($\beta = 0.4$) and 495°C ($\beta = 0.5$), have intensities which are 0.3, 0.4 and 0.5 times total TRM intensity, respectively, for the same applied field.

6.2. *Isothermally Blocked pTRM*

When $T_1 < 482°C$ (e.g., $T_1 = 450°C$ in Figure 10), the picture changes. Walls are blocked at less than their maximum possible displacements. That is, $M(T_2)/M_s(T_2)$, which is maintained during field cooling to T_1, is now $\leq M_{rs}(T_1)/M_s(T_1)$ (indicated by a "virtual" intersection in Figure 10). Thus the walls do not reequilibrate when $H_o \to 0$ at T_1. The resulting pTRM intensity at T_o is $\beta^{-1}(T_2)$ times the IRM intensity at T_2 for the same applied field. The pTRM of this type will be referred to as isothermally blocked. The critical temperature $(T_1)_{crit}$ for the changeover from wall reequilibration to isothermal blocking is found by equating

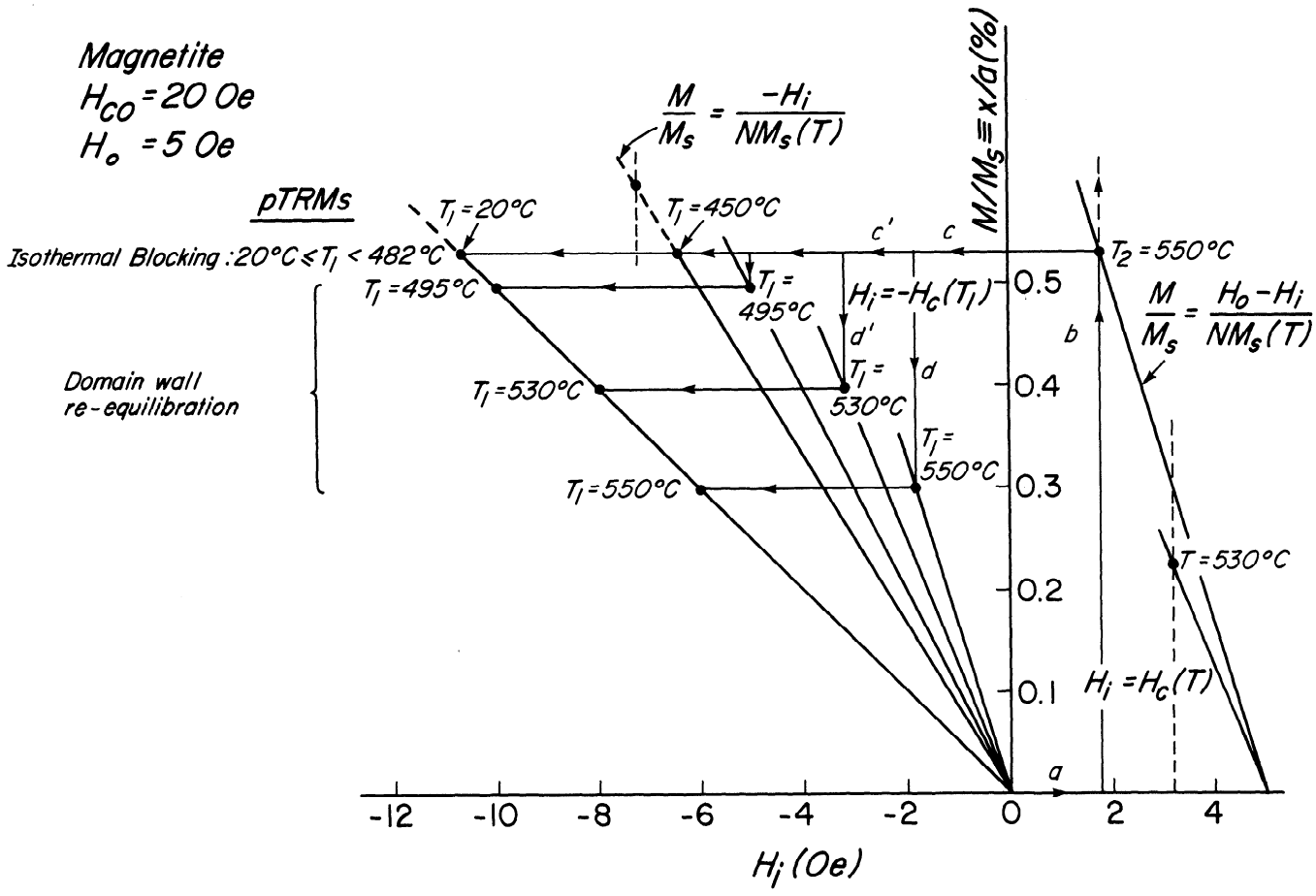

Fig. 10. Simulation of partial TRM acquisition when $H_o = 0.5$ mT is turned on at 550°C during cooling. The blocking temperature of pTRM is 550°C, but $r_H(550°C) > r_o(T_1)$ and the walls reequilibrate if the field is turned off at $T_1 > 482°C$. If $T_1 \leq 482°C$, pTRM remains blocked at $r_H(550°C)$ in cooling to T_o (isothermal blocking). (Note: 1 Oe = 0.1 mT.)

M/M_s at T_2 to M_{rs}/M_s at $(T_1)_{crit}$, which according to (28) gives

$$\frac{H_o - H_c(T_2)}{NM_s(T_2)} = \frac{H_c[(T_1)_{crit}]}{NM_s[(T_1)_{crit}]} \tag{30}$$

Rearranging (30), we have

$$\frac{\beta^{n-1}[(T_1)_{crit}]}{\beta^{n-1}(T_2)} = \frac{H_o}{H_c(T_2)} - 1 \tag{31}$$

As a check, if $(T_1)_{crit} = T_2$, (31) gives $H_o = 2H_c(T_2)$, which is the critical condition derived for IRM acquisition (equation (27)). If $T_2 = 550°C$ ($\beta = 0.3$), so that $H_c(T_2) = 2 \times 0.3^2 = 0.18$ mT, and $H_o = 0.5$ mT, (31) gives $\beta_{crit} = 0.533$ or $(T_1)_{crit} = 482°C$, as stated earlier.

Notice that according to Figure 4, total TRM is always field blocked if $H_o \leq 0.5$ mT (for $H_{co} = 2$ mT and $n = 2$), whereas partial TRM for the same choice of H_{co} and n is isothermally blocked below a temperature $(T_1)_{crit}$ which changes with both T_2 and H_o. For example, applying $H_o = 0.5$ mT at $T_2 = 530°C$ ($\beta = 0.4$) will produce an isothermally blocked partial TRM whatever the temperature T_1 at which $H_o \to 0$. But wall reequilibration will occur over some range of T_1 if H_o is increased to $> 2H_c(T_2) = 2 \times 2 \times 0.4^2 = 0.64$ mT. Thus we anticipate that the field dependence of partial TRM will be more complicated than that of total TRM.

6.3. *Field-Blocked pTRM*

In the cases considered above, there is no field blocking of walls for pTRM during cooling in field H_o. In order to have field blocking, we require that the initial wall displacement $r(T_2) = M(T_2)/M_s(T_2)$ when H_o is turned on be $> r(T_B) = M(T_B)/M_s(T_B)$, which is the field blocking position for TRM. Using (28) to calculate $r(T_2)$ and (10) and (12) to find $r(T_B)$, this gives

$$\frac{H_o - H_c(T_2)}{NM_s(T_2)} \geq \frac{M(T_B)}{M_s(T_B)} = \frac{nH_{co}^{1/n}H_o^{1-1/n}}{(n-1)^{1-1/n}NM_{so}}. \tag{32}$$

Rearranging (32), we have

$$y - \frac{n}{(n-1)^{1-1/n}}y^{1-1/n} - 1 \leq 0, \tag{33}$$

where $y \equiv H_o/H_c(T_2)$. Thus the necessary condition for field blocking to occur during pTRM acquisition is

$$H_o \geq a_n H_c(T_2) \quad \text{or} \quad \beta^n(T_2) \leq \frac{H_o}{a_n H_{co}}. \tag{34}$$

Here a_n is the root of the equation corresponding to the inequality of (33). Numerical values of a_n range from 5.83 when $n = 2$ to 16.6 when $n = 5$ (Table 1).

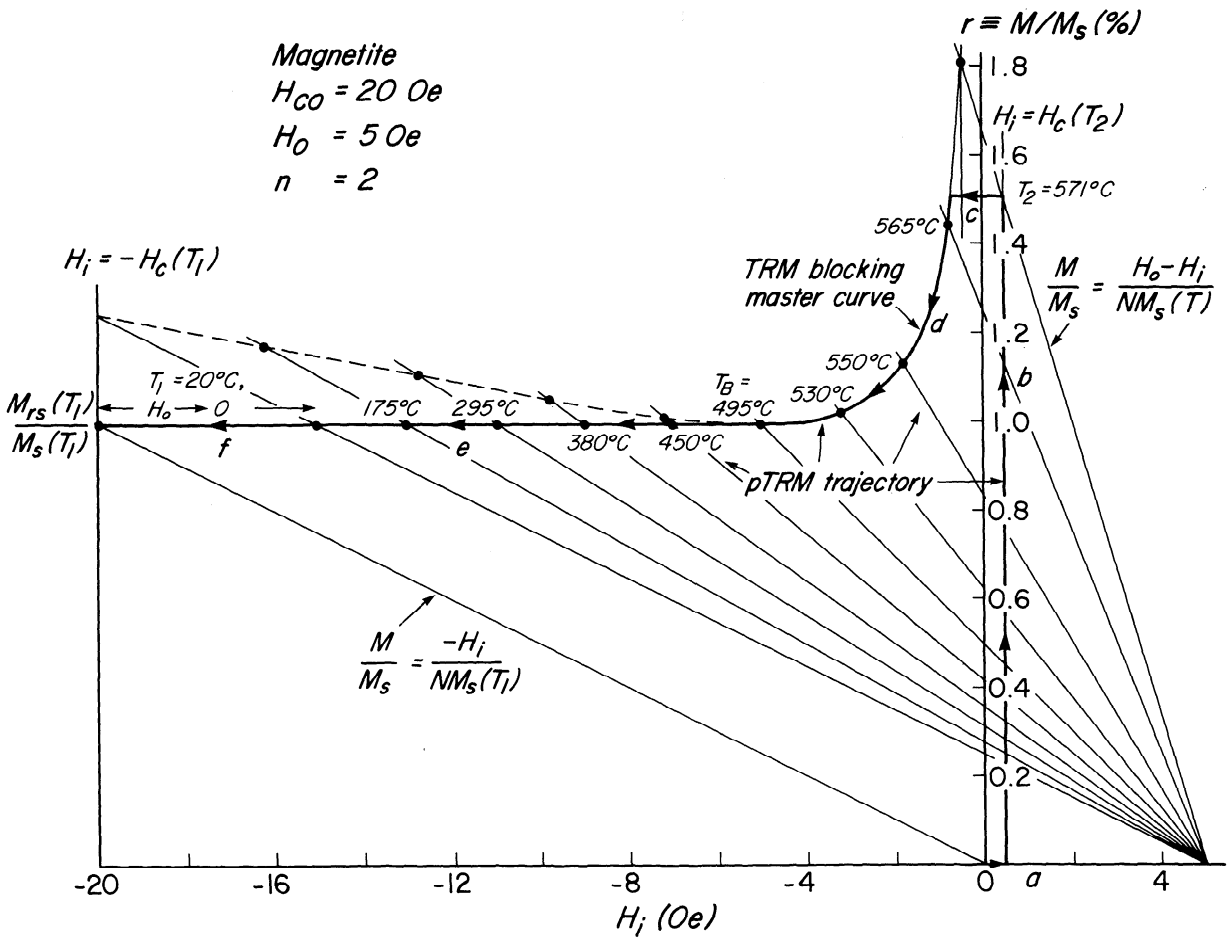

Fig. 11. Simulation of partial TRM acquisition at a higher T_2 (571°C) than in Figure 10. In this case, M/M_s at first follows the minor loop c during field cooling, and then follows part d of the TRM blocking master curve to T_B. The partial TRM in this case has the same intensity and thermal unblocking behavior as total TRM (field blocking). The dashed line is the virtual part of the TRM master curve at temperatures below T_B (cf. Figure 4). (Note: 1 Oe = 0.1 mT.)

An example of the above situation is illustrated in Figure 11. We choose $T_2 = 571°C$. Since $\beta^2(571°C) = 0.15^2 < H_o/(a_n H_{co}) = 0.5/(5.83 \times 2) = 0.043$ from (34), field blocking is possible. When $H_o = 0.5$ mT is applied at 571°C, M follows path a-b to the intersection marked $T_2 = 571°C$. However, 571°C is not the blocking temperature because during field cooling, M follows path c to its intersection with the TRM blocking master curve, defined by descending major loop intersections in Figures 3 and 4. That is, wall reequilibration occurs continuously during cooling and not just when $H_o \rightarrow 0$ at T_1 as in Figure 10. M follows path d to the TRM blocking temperature T_B, at which point the walls are field blocked in the same positions they would occupy in total TRM acquisition.

In order for the walls to remain field blocked when $H_o \rightarrow 0$ at T_1, we require $T_1 \le T'_B$, or $\beta(T_1) \ge \beta(T'_B)$, the thermal demagnetization threshold defined by (23). Using (10) and (23), this gives

$$H_o \le \frac{n-1}{n^{n/(n-1)}} H_c(T_1) \equiv b_n H_c(T_1) \quad \text{or} \quad \beta^n(T_1) \ge \frac{H_o}{b_n H_{co}}. \quad (35)$$

Numerical values of b_n range from 0.250 when $n = 2$ to 0.535 when $n = 5$ (Table 1).

For the example shown in Figure 11, where $n = 2$, $H_{co} = 2$ mT, and $H_o = 0.5$ mT, it can easily be shown that field blocking will not occur if $T_2 < 565°C$ (since the walls will not reequilibrate in cooling below T_2) or if $T_1 > 20°C$ (since the walls will reequilibrate when $H_o \rightarrow 0$ at T_1). Thus total-TRM-like field blocking of pTRMs occurs for a very restricted range of (T_2, T_1) when $n = 2$. It becomes more important for higher values of n as we will show in paper 2.

6.4. *Summary of pTRM Acquired From $T_2 \neq T_c$*

In summary, the room-temperature intensity of the partial TRM acquired between T_2 ($\neq T_c$) and T_1 in a field H_o without any field blocking is

$$M_{ptr}(T_2, T_1, H_o) = 0 \quad \text{if } H_o \le H_c(T_2)$$

$$M_{ptr}(T_2, T_1, H_o) = \frac{H_o - H_{co}\beta^n(T_2)}{N\beta(T_2)}$$

$$\text{if } H_c(T_2) < H_o,\ T_1 \le (T_1)_{crit}$$

$$M_{ptr}(T_2, T_1, H_o) = \frac{H_{co}\beta^{n-1}(T_1)}{N} \quad \text{if } T_1 > (T_1)_{crit}. \quad (36)$$

If $a_n H_c(T_2) < b_n H_c(T_1)$ from (34) and (35), total-TRM-like field blocking may occur at $T_B < T_2$, and the room-temperature intensity of the pTRM is

$$M_{ptr}(T_2, T_1, H_o) = 0 \quad \text{if } H_o \le H_c(T_2)$$

$$M_{ptr}(T_2, T_1, H_o) = \frac{H_o - H_{co}\beta^n(T_2)}{N\beta(T_2)}$$

$$\text{if } H_c(T_2) < H_o \le a_n H_c(T_2)$$

$$M_{ptr}(T_2, T_1, H_o) = \frac{nH_{co}^{1/n}H_o^{1-1/n}}{(n-1)^{1-1/n}N}$$

$$\text{if } a_n H_c(T_2) < H_o \le b_n H_c(T_1)$$

$$M_{ptr}(T_2, T_1, H_o) = \frac{H_{co}\beta^{n-1}(T_1)}{N} \quad \text{if } b_n H_c(T_1) < H_o. \quad (37)$$

TABLE 1. Values of the Critical Field Coefficients a_n and b_n From (34) and (35)

n	a_n	b_n
2	5.828	0.250
3	9.444	0.385
4	13.04	0.473
5	16.64	0.535

The first alternatives in (36) and (37) correspond to trapping of walls in their initial (demagnetized) positions, the second to isothermal blocking at T_2, and the third in (37) to field blocking at $T_B < T_2$. The last alternatives in (36) and (37) correspond to wall reequilibration at T_1. Rather than calculating the conditions explicitly in either (36) or (37), it is often quicker to compute the alternative values of pTRM intensities and choose whichever is smallest. We will use the results of (36) in the following section to test the additivity law of partial TRMs.

7. ADDITIVITY OF PARTIAL TRMS

The previous section considered only pTRMs acquired from an upper temperature T_2 at which the saturation field $NM_s(T_2)$ was $> H_o$. For fields ≤ 0.5 mT, this is the situation even if T_2 is within a degree of T_c. However, to test the law of additivity of pTRMs, we need to calculate also partial TRM acquired between T_c and a temperature $T_1 \neq T_o$. In this case, the walls are initially at their limiting positions even for small H_o values, and we descend the major loop during cooling and when $H_o \rightarrow 0$ at T_1.

As outlined in section 4.1, there are two possibilities for the partial TRM measured at T_o

$$M_{ptr}(T_c, T_1, H_o) = \frac{nH_{co}^{1/n}H_o^{1-1/n}}{(n-1)^{1-1/n}N} \quad T_1 \le T'_B$$

$$M_{ptr}(T_c, T_1, H_o) = \frac{H_c(T_1)}{N\beta(T_1)} = \frac{H_{co}\beta^{n-1}(T_1)}{N} \quad T_1 > T'_B, \quad (38)$$

where T'_B is given by (23) and $M_{tr}(T_o)$ is given by (13). The first alternative corresponds to field blocking and the second to wall reequilibration at T_1. Again it is usually quicker to compute both alternatives and choose the smaller, rather than calculating T'_B explicitly. We can see from this discussion that $(T_1)_{crit}$ calculated in the previous section is a generalization of T'_B for the case when $T_2 \neq T_c$ and minor loops are traversed during pTRM acquisition.

Table 2 gives an example of a total TRM and some examples of partial TRMs calculated using (13), (36) and (38). The law of additivity of partial TRMs, as stated by *Thellier* [1938], is only very approximately obeyed for multidomain grains. The sum of pTRMs acquired in adjacent nonoverlapping (T_2, T_1) intervals spanning the (T_c, T_o) range is never exactly equal to the total TRM. For the examples that we calculated, ΣpTRMs ranged from a low of 0.62 × TRM to a high of 1.37 × TRM. We made no attempt to determine the maximum possible deviation from the additivity law; however, merely increasing the number of pTRMs in the sum did not systematically increase or decrease the deviation.

An individual single-domain grain, or an ensemble of identical grains with the same microcoercivity, has a narrow blocking temperature interval outside which it cannot acquire partial TRM. Additivity of pTRMs is a natural consequence of the fact that each grain or ensemble contributes one and only one partial TRM

TABLE 2. Some Sample Calculations Testing the Additivity of Partial TRMs, $M_{ptr}(T_2, T_1, H_o)$

Type	T_2, °C	T_1, °C	$M_r(T_o)/M_{so}$, %	Regime
TRM	580	20	0.995	Field blocking/wall reequilibration (critical condition)
pTRM	580	530	0.398	Wall reequilibration
pTRM	530	20	0.224	Isothermal blocking
ΣpTRMs			0.622	
pTRM	580	550	0.298	Wall reequilibration
pTRM	550	20	0.531	Isothermal blocking
ΣpTRMs			0.829	
pTRM	580	565	0.199	Wall reequilibration
pTRM	565	20	0.995	Wall reequilibration
ΣpTRMs			1.194	
pTRM	580	565	0.199	Wall reequilibration
pTRM	565	530	0.398	Wall reequilibration
pTRM	530	20	0.224	Isothermal blocking
ΣpTRMs			0.821	
pTRM	580	572	0.149	Wall reequilibration
pTRM	572	565	0.199	Wall reequilibration
pTRM	565	550	0.298	Wall reequilibration
pTRM	550	530	0.398	Wall reequilibration
pTRM	530	20	0.224	Isothermal blocking
ΣpTRMs			1.268	
pTRM	580	572	0.149	Wall reequilibration
pTRM	572	565	0.199	Wall reequilibration
pTRM	565	550	0.298	Wall reequilibration
pTRM	550	530	0.398	Wall reequilibration
pTRM	530	515	0.224	Isothermal blocking
pTRM	515	495	0.105	Isothermal blocking
pTRM	495	450	0	Trapped walls
pTRM	450	20	0	Trapped walls
ΣpTRMs			1.373	

Parameters assumed are $H_o = 0.5$ mT, $H_{co} = 2$ mT, $n = 2$.

to the total TRM. A multidomain grain with a single microcoercivity, on the other hand, can acquire partial TRMs over many different temperature intervals, each pTRM corresponding to a different set of wall displacements, and there is no a priori reason why these pTRMs should be additive.

8. THERMAL DEMAGNETIZATION OF PARTIAL TRM

There are three situations to be considered.

1. M_{ptr} is field blocked at the TRM blocking temperature T_B and remains blocked at T_1 when $H_o \to 0$, that is, the third alternative in (37) or the first in (38). It has the same intensity and is in every way indistinguishable from total TRM. The partial TRM will demagnetize in the way outlined in section 4 and Figure 8: continuous reequilibration of walls occurs and thus $M_r(T) \propto \beta^{n-1}(T)$ for $T > T'_B$ (cf. equation (25)).

2. M_{ptr} reequilibrates at T_1 during cooling, that is, the last alternatives in (36) and (37) and the second in (38). In zero-field heating, reequilibration of walls occurs only above T_1, and $M_r(T) \propto \beta^{n-1}(T)$ for $T > T_1$.

3. M_{ptr} is isothermally blocked at T_2, that is, the second alternatives in (36) and (37). Walls will not begin to reequilibrate during heating until T reaches $(T_1)_{crit}$, above which $M_r(T) \propto \beta^{n-1}(T)$.

In all cases, partial TRMs should be thermally demagnetized in proportion to $\beta^{n-1}(T)$ (stepwise heating) or $\beta^n(T)$ (continuous heating) above a threshold temperature T_{crit} at which walls begin to be driven back by the internal demagnetizing field $H_d = -NM_r(T)$ against the diminishing resistance $H_c(T)$. Quantitatively, in stepwise thermal demagnetization, the fraction of partial TRM remaining after heating to T (all measurements made after zero-field cooling to T_o) is

$$\frac{M_{ro}(T)}{M_{ptr}(T_o)} = \frac{\beta^{n-1}(T)}{\beta^{n-1}(T_{crit})} \qquad T > T_{crit}. \tag{39}$$

Equation (39) resembles (25) for the stepwise thermal demagnetization of total TRM, except that T_{crit} for the onset of demagnetization can be variously T'_B (case 1), T_1 (case 2), and $(T_1)_{crit}$ (case 3).

For partial TRMs acquired from $T_2 \neq T_c$, the onset temperature for demagnetization is much higher than for total TRM or most partial TRMs acquired from T_c. Compare, for example, Figures 8, 12, and 13: when $H_o = 0.5$ mT, total TRM begins to demagnetize in the first heating step above T_o, whereas partial TRMs demagnetize only above 482°C or higher. Furthermore, Table 2 demonstrates that for the same parameters used to generate Figures 8, 12, and 13, $M_{ptr} = 0$ if $T_2 \leq 495$°C, because $H_o < H_c(T_2)$ and walls cannot escape from their initial demagnetized positions (equations (37) and (38)). Thus when $n = 2$ there is no possibility of blocking or unblocking temperatures much below 500°C for a partial TRM with $T_2 \neq T_c$. For smaller fields, ≈ 0.1 mT or less, pTRM blocking and unblocking temperatures are even higher.

9. DISCUSSION

9.1. *Total TRM and Partial TRM Acquired From T_c to T_1*

Total and partial TRM acquired in cooling in an applied field from above the Curie point have a different blocking process from partial TRM in which the field is first applied below the Curie point. The internal demagnetizing field $\mathbf{H}_d(T) = -N\mathbf{M}_s(T)$ only drops below ≈ 0.1 mT within about 1°C of T_c. Thus if $\mathbf{H}_o$ is applied at T_c, it will move walls to their limiting positions and the grain will begin its cooling in a state of near-saturation magnetization. Walls reequilibrate their positions almost continuously during cooling in response to the growing restoring force of $\mathbf{H}_d(T)$ until they are driven back to the minimum displacements permitted by the growth of wall pinning, represented by $H_c(T)$.

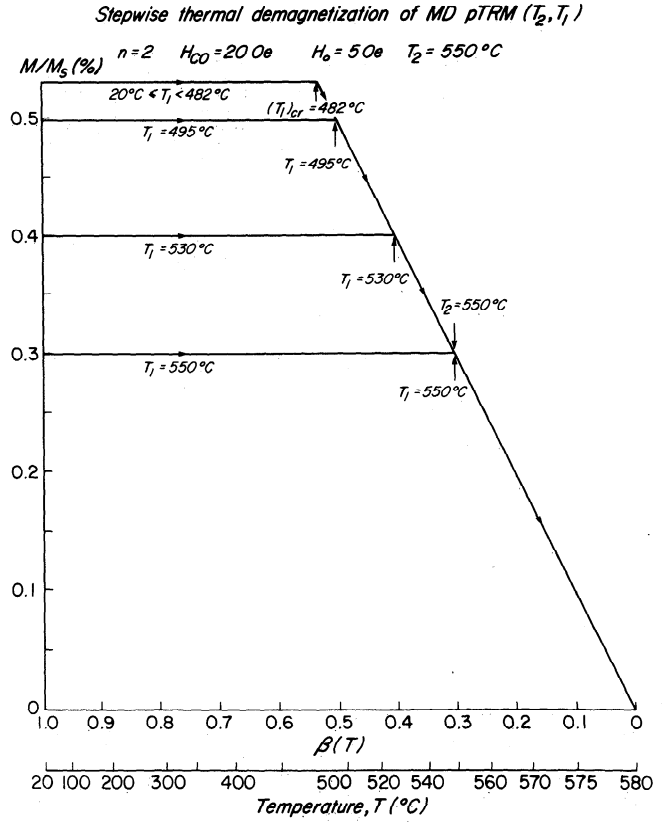

Fig. 12. Simulated thermal demagnetization of the partial TRMs modeled in Figure 10. The pTRM is unaffected by heating up to $(T_1)_{crit}$ (isothermally blocked pTRMs) or T_1 (reequilibrated pTRMs), above which the thermal demagnetization master curve is followed (cf. Figure 7). Notice that cooling to lower T_1 before removing the field increases the pTRM intensity, but the additional pTRM unblocks at low temperatures during heating. (Note: 1 Oe = 0.1 mT.)

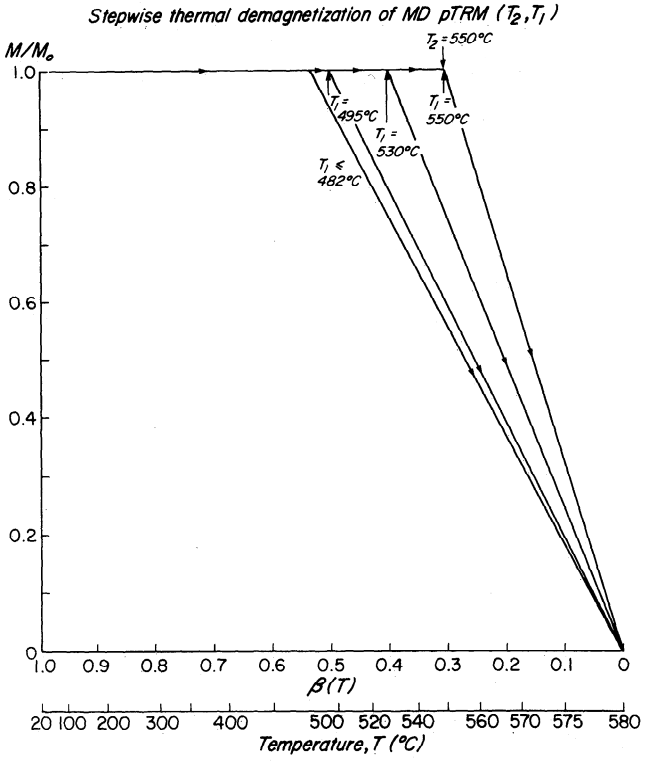

Fig. 13. The demagnetization curves of Figure 12 replotted in normalized form, emphasizing the fact that pTRMs with high acquisition temperatures also have high unblocking temperatures, much higher than those of total TRM for the same H_o (cf. Figure 8).

The balance between $\mathbf{H}_o$, $\mathbf{H}_d$, and H_c is achieved at the blocking temperature T_B (equation (10)), which is different for each value of H_o and H_{co}.

The walls remain pinned until $H_o \rightarrow 0$ at T_1 (partial TRM) or T_o (total TRM), at which point they may reequilibrate to reduce M_{ptr} to $M_{rs}(T_1)$ or M_{tr} to $M_{rs}(T_o)$. This conditional blocking, in which walls readjust their positions to reduce the magnetization to the saturation remanence when the applied field is removed, is what we call wall reequilibration TRM. It occurs when H_o/H_c exceeds a critical value (equation (19) for TRM) or T_B is below a critical value $(T_B)_{min}$ (equation (20)).

If walls do not reequilibrate when $H_o \rightarrow 0$, we have field-blocked TRM. The easiest test is to calculate the highest temperature T'_B at which walls remain blocked when $H_o \rightarrow 0$, using (23). If $T'_B \geq T_o$ or T_1 as the case may be, the TRM or partial TRM is field blocked and has a room-temperature intensity given by (13). Otherwise, wall reequilibration occurs at T_o or T_1, and TRM or partial TRM intensity equals the saturation remanence $M_{rs}(T) = H_c(T)/N$ (scaled up by a factor $\beta^{-1}(T_1)$ in cooling from T_1 to T_o in the case of pTRM).

There is an alternative to field-blocked and reequilibrated TRMs. For sufficiently small fields, T_B is so high that the energy barrier to wall motion can be overcome by thermal fluctuations, in exact analogy to the situation in single-domain grains. Then the TRM is thermally blocked below a lower thermal fluctuation blocking temperature T_{Bf} given by (14), and TRM intensity is proportional to H_o according to (16).

9.2. *Field Dependence of TRM Intensity*

Thus there are three regions in the field response of TRM. For a fixed H_{co}, TRM intensity is proportional to H_o for weak fields ($\leq$0.2 mT), varies as a power <1 of H_o for intermediate fields and

is independent of H_o for strong fields. These regions correspond to thermally blocked, field-blocked, and wall reequilibration TRM, respectively. Measured M_{tr} versus H_o data do fall into three regions with approximately these properties (Figure 6) [also see *Dunlop and Waddington*, 1975; *Tucker and O'Reilly*, 1980].

The critical values of H_o separating the regions are given by (17) and (19) (the latter was not considered by *Néel* [1955]). The upper critical field is proportional to H_{co}, so that for real rocks with a distribution of microcoercivities, the saturation of TRM will be gradual, not abrupt. The lower critical field does not depend on microcoercivity (i.e., barrier heights or slopes) but does depend on activation volume V (i.e., on the distance the wall moves in one Barkhausen jump). Real rocks will have a distribution of V as well as H_{co}, and so the onset of nonlinear TRM will probably be gradual as well.

9.3. *Thermal Demagnetization*

There are three corresponding regions in the thermal demagnetization of TRM or pTRM. During zero-field heating above T_o, TRM or pTRM intensity remains constant (apart from a reversible decrease due to $M_s(T)$) up to either T_1 or T'_B, whichever is greater. In this T range, the TRM or pTRM remains essentially field-blocked. T_1 or T'_B is the lowest unblocking temperature T_{UB} of the remanence, which with further heating continuously reequilibrates (through wall jumps) to values $M_{rs}(T) = H_c(T)/N$ up to the ultimate demagnetization temperature T_D at which all remanence vanishes. This is the wall reequilibration region. T_D is always equal to T_{Bf}, because above T_{Bf}, any remanence is thermally unblocked. However, in contrast to the unblocking of single-domain grains, $T_D = T_{Bf}$ is always very close to T_c and may not always be distinguishable from T_c experimentally.

The situation in thermal demagnetization is therefore that TRM or pTRM with a single T_B during in-field cooling demagnetizes over a broad T_{UB} range, corresponding to continuous field reequilibration. The lowest T_{UB} corresponds to either the lower temperature T_1 of the pTRM or T'_B and the highest approaches T_c. In the case of wall reequilibration TRM, thermal demagnetization occurs over the entire range (T_o, T_c). This behavior is very different from that of single-domain grains but matches experimental observations. A detailed comparison with experiment will be made in paper 2 [*Xu and Dunlop*, this issue].

9.4. *Partial TRM Acquired From $T_2 \neq T_c$*

Now we turn to partial TRM in which H_o is applied at a temperature T_2 which is below T_c (even slightly below will suffice). Starting now from a nearly demagnetized state, since $H_o \ll NM_s(T_2)$, if $H_o < H_c(T_2)$, the walls remain pinned and no pTRM is produced. If $H_o \geq H_c(T_2)$, walls will be driven out of their local wells but will remain much closer to the demagnetized state than for TRM or pTRM in which H_o is applied at T_c. With falling temperature in a constant applied field, the total energy would be lowered if the walls returned even closer to the demagnetized state, but H_d is too small to drive the walls back across local barriers in E_w. Equivalently, M cannot descend the ascending major loop. Consequently, the pTRM is isothermally blocked at T_2 and remains blocked in cooling to lower temperatures. (An exception occurs if $T_2 > T_{Bf}$, in which case thermal blocking occurs at T_{Bf}).

If $a_n H_c(T_2) < H_o$ (equation (34)), a decrease in $H_c(T)$ (relative to $H_d(T)$) with cooling in H_o can result in unblocking of the walls from their isothermally blocked positions, and the walls may then be field blocked at T_B ($< T_2$) as in Figure 11. The resulting pTRM in this case has the same properties as total TRM.

If the lower temperature T_1 is less than $(T_1)_{crit}$ (equation (31)) for the isothermally blocked pTRM or $H_o \leq b_n H_c(T_1)$ (equation (35)) for the field blocked pTRM, the walls remain blocked throughout cooling to T_1 in H_o and when $H_o \rightarrow 0$ at T_1. The normalized wall displacement $r = x/a$, which is also the normalized magnetization $M(T)/M_s(T)$, remains fixed at the value it had at either T_2 for isothermal blocking or T_B for field blocking. The room-temperature pTRM intensity is higher by virtue of the reversible increase in $M_s(T)$ between T_1 and T_o and is given by the second alternative of (36) or (37) for isothermal blocking or the third of (37) for field blocking.

On the other hand, if $T_1 > (T_1)_{crit}$ for the isothermally blocked pTRM or $H_o > b_n H_c(T_1)$ for the field-blocked pTRM, the walls will be driven back when $H_o \rightarrow 0$ at T_1. This wall reequilibration pTRM will be equal to $M_{rs}(T_1)$, if measured at T_1, or a factor $\beta^{-1}(T_1)$ larger than this at T_o (final alternative of (36) or (37)).

In the acquisition of pTRM, there are thermal blocking, isothermal blocking, field blocking and wall reequilibration regions, but the boundaries depend on T_2 and T_1 as well as on H_o and H_{co}. If T_2 is close to T_c, the pTRM will be thermally blocked at $T_{Bf} < T_2$. Otherwise, the pTRM is isothermally blocked at T_2 or field-blocked at the TRM blocking temperature T_B. If T_1 is well below T_2, the pTRM will be $< M_{rs}(T_1)$ and will remain isothermally blocked or field blocked when the field is removed at T_1 and during zero-field cooling to T_o. If T_1 is close to T_2, then $M_{rs}(T_1)$ will be small and the pTRM will reequilibrate downward to this value when $H_o \rightarrow 0$. The general tendency is for pTRMs acquired over narrow (T_2, T_1) intervals to be wall reequilibrated, while pTRMs with wide (T_2, T_1) intervals will be isothermally blocked or field blocked.

Because of the interplay between the parameters H_o, H_{co}, T_2, and T_1, the field dependence of partial TRM is more complicated than the field response of total TRM. Some specific cases will be dealt with in paper 2.

9.5. *Thermal Demagnetization*

The thermal demagnetization of the pTRM with $T_2 \neq T_c$ follows the same principles as the thermal demagnetization of total TRM and pTRM with $T_2 = T_c$. During zero-field heating, pTRM intensity remains constant (stepwise cleaning) or decreases reversibly with $M_s(T)$ (continuous demagnetization) as long as the walls remain blocked, that is, up to a threshold temperature T_{crit}, which is T_1 for reequilibrated pTRM, T'_B for field-blocked pTRM or $(T_1)_{crit}$ for isothermally blocked pTRM. Above this threshold, the walls reequilibrate almost continuously and pTRM intensity drops in proportion to $H_c(T)$ (continuous) or $H_c(T)/M_s(T)$ (stepwise cleaning) up to $T_D = T_{Bf}$, which is in practice close to T_c.

Notice that the threshold temperature for the pTRM acquired from $T_2 \neq T_c$ may be much higher than for pTRM acquired from T_c or total TRM (compare the 0.5-mT curves in Figures 8 and 13). In fact, for the same H_o, the high unblocking temperature parts of all three types of remanence have identical intensities (cf. Figure 12). The "excess" room-temperature intensity of TRM and pTRM acquired from T_c is completely removed in low-temperature heatings and would not contribute to the stable part of natural remanence isolated by thermal demagnetization.

Table 3 summarizes the formulas needed to calculate intensities and thermal demagnetization curves of partial and total TRMs. Rather than calculating values for the various critical blocking and unblocking temperatures, it is computationally convenient and quicker to calculate magnetization values for all possible options (thermal blocking, isothermal blocking, field blocking,

TABLE 3*a*. Summary of Formulas for Calculating Total and Partial TRM Intensities and Thermal Demagnetization Curves: Total TRM, $M_{tr}(T_c, T_o, H_o)$, Measured at T_o

Process and Formula(s)	Range of Validity	Regime
$M_{tr} = [H_{co}^{1/n}/NH_f(T_{Bf})^{1/n}]H_o$	$T_{Bf} \le T_B$	Thermal blocking
$M_{tr} = [n/(n-1)^{1-1/n}]H_{co}^{1/n}H_o^{1-1/n}/N$	$T_{Bf} > T_B$ and $T_o \le T'_B$	Field blocking
$M_{tr} = M_{rs}(T_o) = H_{co}/N$	$T'_B < T_o$	Wall reequilibration

$\beta(T_B) = [H_o/(n-1)H_{co}]^{1/n}$, $\beta(T'_B) = n^{1/(n-1)}\beta(T_B)$, $\beta(T_{Bf}) = [H_f(T_{Bf})/H_{co}]^{1/n}$, and $H_f(T) = kT(\log f_o t)/[2VM_s(T)]$.

TABLE 3*b*. Summary of Formulas for Calculating Total and Partial TRM Intensities and Thermal Demagnetization Curves: Partial TRM, $M_{ptr}(T_c, T_1, H_o)$, Measured at T_o

Process and Formula(s)	Range of Validity	Regime
$M_{ptr} = [H_{co}^{1/n}/NH_f(T_{Bf})^{1/n}]H_o$	$T_{Bf} \le T_B$	Thermal blocking
$M_{ptr} = [n/(n-1)^{1-1/n}]H_{co}^{1/n}H_o^{1-1/n}/N$	$T_{Bf} > T_B$ and $T_1 \le T'_B$	Field blocking
$M_{ptr} = \beta^{n-1}(T_1)H_{co}/N$	$T'_B < T_1$	Wall reequilibration

TABLE 3*c*. Summary of Formulas for Calculating Total and Partial TRM Intensities and Thermal Demagnetization Curves: Partial TRM, $M_{ptr}(T_2 \ne T_c, T_1, H_o)$, Measured at T_o $(a_n H_c(T_2) > b_n H_c(T_1))$

Process and Formula(s)	Range of Validity	Regime
$M_{ptr} = 0$	$H_o \le H_c(T_2)$	Walls trapped
$M_{ptr} = [H_o - H_{co}\beta^n(T_2)]/N\beta(T_2)$	$H_o > H_c(T_2)$ and $T_1 \le (T_1)_{crit}$	Isothermal blocking
$M_{ptr} = \beta^{n-1}(T_1)H_{co}/N$	$T_1 > (T_1)_{crit}$	Wall reequilibration

The parameter a_n can be found from (34) and $b_n = (n-1)/n^{n(n-1)}$ (see Table 1), and $\beta^{n-1}[(T_1)_{crit}]/\beta^{n-1}(T_2) = [H_o/\beta^n(T_2)H_{co}] - 1$.

TABLE 3*d*. Summary of Formulas for Calculating Total and Partial TRM Intensities and Thermal Demagnetization Curves: Partial TRM, $M_{ptr}(T_2 \ne T_c, T_1, H_o)$, Measured at T_o $(a_n H_c(T_2) \le b_n H_c(T_1))$

Process and Formula(s)	Range of Validity	Regime
$M_{ptr} = 0$	$H_o < H_c(T_2)$	Walls trapped
$M_{ptr} = [H_o - H_{co}\beta^n(T_2)]/N\beta(T_2)$	$H_c(T_2) < H_o \le a_n H_c(T_2)$	Isothermal blocking
$M_{ptr} = [n/(n-1)^{1-1/n}]H_{co}^{1/n}H_o^{1-1/n}/N$	$a_n H_c(T_2) < H_o \le b_n H_c(T_1)$	Field blocking
$M_{ptr} = \beta^{n-1}(T_1)H_{co}/N$	$H_o > b_n H_c(T_1)$	Wall reequilibration

TABLE 3*e*. Summary of Formulas for Calculating Total and Partial TRM Intensities and Thermal Demagnetization Curves: Thermal Demagnetization of TRM or pTRM (Denoted by M_o)

Process and Formula(s)		Range of Validity	Regime
Stepwise	Continuous		
$M_{ro}(T)/M_o = 1$	$= \beta(T)$	$T \le T_{crit}$	Walls blocked
$M_{ro}(T)/M_o = \beta^{n-1}(T)/\beta^{n-1}(T_{crit})$	$= \beta^n(T)/\beta^{n-1}(T_{crit})$	$T_{crit} < T \le T_{Bf}$	Continuous wall reequilibration
$M_{ro}(T)/M_o = 0$	$= 0$	$T > T_{Bf}$	Thermally unblocked

$T_{crit} = T'_B$ for field blocked M_{tr} or M_{ptr}, $T_{crit} = T_1$ for wall reequilibration M_{tr} or M_{ptr}, and $T_{crit} = (T_1)_{crit}$ for isothermally blocked M_{ptr}.

and wall reequilibration). The grain will always choose the lowest magnetization.

10. CONCLUSIONS

1. We have extended the *Néel* [1955] model of total TRM in a multidomain grain with a single microcoercivity H_{co} and no screening by soft walls to treat the acquisition of partial TRMs and the thermal demagnetization of total and partial TRMs.

2. There are in general three regimes in the acquisition of TRM and pTRM acquired from T_c: (1) thermal blocking (small H_o/H_{co} and activation volume V, high blocking temperature), in which thermal energy becomes inadequate to unpin walls; (2) field blocking (intermediate H_o/H_{co} and blocking temperature T_B), in which walls reequilibrate from T_c to T_B and are pinned at T_B by H_c in the subsequent cooling; and (3) wall reequilibration (large H_o/H_{co}, low blocking temperature), in which initially blocked walls unpin when $H_o \rightarrow 0$ at either T_o or T_1. There is an additional regime in the acquisition of pTRM acquired from $T_2 \neq T_c$: isothermal blocking (small H_o/H_{co}, blocking temperature = T_2), in which the internal demagnetizing field H_d cannot unpin walls from their initially blocked positions at T_2.

3. When H_o is applied at T_c, it moves walls to a near-saturation state. As T and eventually H_o decrease, M is driven down the descending major loop by H_d; this is the case modeled by *Néel* [1955]. However, when H_o is applied at a temperature T_2 even slightly lower than T_c, the pTRM process is quite different. M is driven up the ascending major loop (usually from a near-demagnetized state) and traverses a minor loop when T and then H_o decrease. This case was not considered by *Néel* [1955], although it has recently been independently discovered by *Shcherbakov et al.* [1993].

4. The partial TRM acquired from $T_2 \neq T_c$ is usually considerably less intense than the partial TRM acquired from T_c, but it has uniformly high unblocking temperatures. Thermal demagnetization will isolate the same high-T_{UB} residual magnetization in either type of pTRM or in a total TRM.

5. Although total and partial TRM block at a relatively sharp blocking temperature, they unblock over a broad range of T_{UB} values, extending essentially to T_c. The minimum T_{UB} is lowest for total TRM, generally higher for pTRM acquired from T_c, and highest for pTRM acquired from $T_2 \neq T_c$. If wall reequilibration has occurred during acquisition, TRM begins to demagnetize immediately above T_o, and pTRMs begin to demagnetize at T_1. Field-blocked TRM and field or isothermally blocked pTRM begin to demagnetize at somewhat higher temperatures than T_o or T_1.

6. Remanence intensity decreases in proportion to $H_c(T)$ in continuous thermal demagnetization or $\propto H_c(T)/M_s(T)$ in stepwise cleaning for $T > T_{crit}$ (= the minimum T_{UB}).

7. A grain with a single microcoercivity H_{co} can acquire partial TRMs over many different (T_2, T_1) ranges. These partial TRMs are not independent and their intensities are only very approximately additive. For the calculations of Table 2, the sum of the pTRMs ranged from 0.62 to 1.37 times TRM.

APPENDIX: THERMAL VARIATION OF SATURATION MAGNETIZATION $M_s(T)$

For the calculations in the present paper, we used experimental values of $M_s(T)$ measured for magnetite by *Pauthenet and Bochirol* [1951]. For intensive computations, such as the numerical modeling in paper 2 [*Xu and Dunlop*, this issue], an analytic approximation like

$$\frac{M_s(T)}{M_{so}} = \left[\frac{T_c - T}{T_c - T_o}\right]^{\gamma} \tag{40}$$

is more convenient. The γ in (40) is a constant determined by a best fit to measured values of $M_s(T)$. For Fe_3O_4, $\gamma \approx 0.43$ [e.g., *Worm et al.*, 1988]. The two are compared in Figure 14.

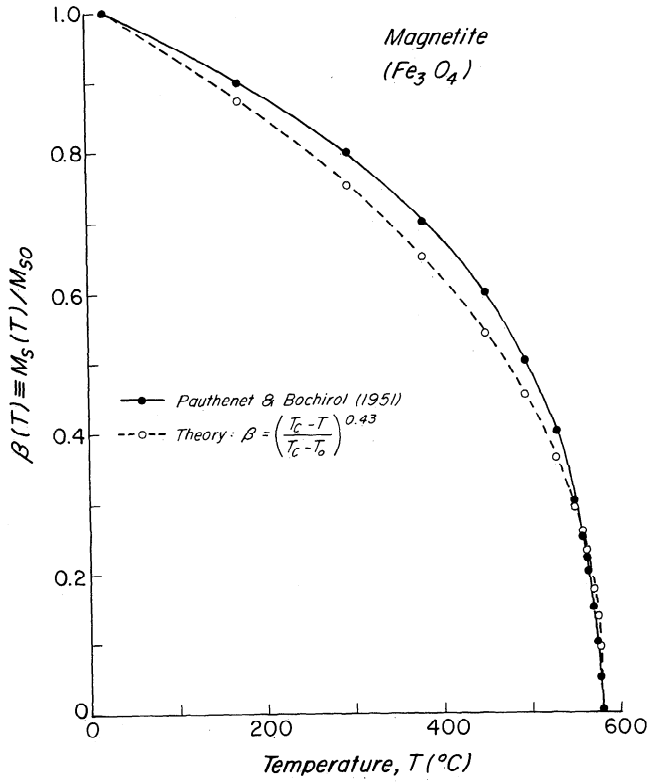

Fig. 14. Two versions of $\beta(T)$ for magnetite. Data measured by *Pauthenet and Bochirol* [1951] were used for calculations in the present paper, while an analytic approximation based on molecular field theory (dashed curve) is convenient for intensive computations, such as those in companion paper 2.

NOTATION

- a half grain size or limiting wall displacement.
- h_c microcoercivity.
- $f(h_c)$ distribution of microcoercivities (paper 2).
- $m, m(h_c)$ magnetization associated with displacement of a single wall with microcoercivity h_c (paper 2).
- n exponent to $M_s(T)$ that describes the temperature variation of $H_c(T)$, i.e., $H_c(T) \propto M_s^n(T)$.
- r wall displacement normalized to grain size, that is, $r = x/a$.
- r_{min} minimum normalized wall displacement, achieved at T_B.
- r_o, r_H normalized wall displacements in zero applied field and in $\mathbf{H}_o$, respectively.
- x wall displacement.
- A wall area ($= 4a^2$).
- E total magnetic energy of a grain.
- E_w domain wall energy.
- $\mathbf{H}_o$ external applied magnetic field.
- $(H_o)_{crit}$ critical H_o above which one has reequilibrated instead of field-blocked TRM or pTRM.

$(H_o)_f$ critical H_o below which one has thermally blocked instead of field-blocked TRM or pTRM.
H_c bulk coercive force (numerically equal to h_c in the case of identical symmetrical E_w barriers or to the mean of the distribution $f(h_c)$ for irregular barriers).
H_{co} room temperature value of H_c.
$\mathbf{H}_d$ internal demagnetizing field ($= -N\mathbf{M}$).
H_f thermal fluctuation field.
$\mathbf{H}_i$ total internal magnetic field ($= \mathbf{H}_o + \mathbf{H}_d$).
$\mathbf{M}$ magnetization (magnetic moment per unit volume) of a grain.
M_{ptr} partial TRM intensity (per unit volume) of a grain.
M_r remanent magnetization.
M_{ro} remanence at room temperature.
M_{rs} saturation remanence.
M_s saturation magnetization.
M_{so} room temperature value of M_s.
M_{tr} total TRM intensity (per unit volume).
N demagnetizing factor (taken to be 1/3 in SI or $4\pi/3$ in cgs units in numerical calculations).
T temperature.
T_o room temperature.
T_1 lower temperature at which $\mathbf{H}_o$ is turned off in pTRM acquisition.
$(T_1)_{crit}$ critical T_1 below which there is a changeover from wall reequilibration to isothermal blocking of pTRM.
T_2 upper temperature at which $\mathbf{H}_o$ is turned on in pTRM acquisition.
T_c Curie temperature.
T_B blocking temperature of field-blocked TRM or pTRM.
T'_B temperature at which walls first begin to unblock during thermal demagnetization of TRM.
T_{Bf} thermal fluctuation blocking temperature.
$(T_B)_{min}$ minimum T_B below which one has reequilibrated instead of field-blocked TRM or pTRM.
T_{UB} unblocking temperature; for a multidomain grain, a temperature range, of which the minimum is T'_B.
T_D ultimate demagnetizing temperature at which all remanence vanishes.
α magnetostatic screening factor (paper 2).
$\beta(T)$ ratio $M_s(T)/M_{so}$.
γ exponent of $(T_c - T)$ that describes the temperature dependence of $M_s(T)$, that is, $M_s(T) \propto (T_c - T)^\gamma$.

Acknowledgments. We thank Wyn Williams, Susan Halgedahl, and Lisa Tauxe for their critical comments. This research has been supported by the Natural Sciences and Engineering Research Council of Canada through operating grant A7709.

REFERENCES

Bolshakov, A.S., and V.V. Shcherbakova, Thermomagnetic criteria for ferrimagnetic domain structure, *Izv. Akad. Nauk SSSR, Ser. Fiz. Zemli, 2,* 38-47, 1979.

Day, R., TRM and its variation with grain size, *J. Geomagn. Geoelectr., 29,* 233-265, 1977.

Dunlop, D.J., Theory of the magnetic viscosity of lunar and terrestrial rocks, *Rev. Geophys., 11,* 855-901, 1973.

Dunlop, D.J., Field dependence of magnetic blocking temperature: Analog tests using coercive force data, *J. Geophys. Res., 87,* 1121-1126, 1982.

Dunlop, D.J., On the demagnetizing energy and demagnetizing factor of a multidomain ferromagnetic cube, *Geophys. Res. Lett., 10,* 79-82, 1983.

Dunlop, D.J., and E.D. Waddington, The field dependence of thermoremanent magnetization in igneous rocks, *Earth Planet. Sci. Lett., 25,* 11-25, 1975.

Everitt, C.W.F., Thermoremanent magnetization. III. Theory of multidomain grains, *Philos. Mag., 7,* 599-616, 1962.

Gaunt, P.J., The frequency constant for thermal activation of a ferromagnetic domain wall, *J. Appl. Phys., 48,* 4370-4374, 1977.

Halgedahl, S.L., Domain pattern observations in rock magnetism: progress and problems, *Phys. Earth Planet. Inter., 46,* 127-163, 1987.

Halgedahl, S.L., Magnetic domain patterns observed on synthetic Ti-rich titanomagnetite as a function of temperature and in states of thermoremanent magnetization, *J. Geophys. Res., 96,* 3943-3972, 1991.

Hartstra, R.L., High-temperature characteristics of a natural titanomagnetite, *Geophys. J. R. Astron. Soc., 71,* 455-476, 1982.

Hartstra, R.L., TRM, ARM and Isr of two natural magnetites of MD and PSD grain size, *Geophys. J. R. Astron. Soc., 73,* 719-737, 1983.

Heider, F., D.J. Dunlop, and N. Sugiura, Magnetic properties of hydrothermally recrystallized magnetite crystals, *Science, 236,* 1287-1289, 1987.

Heider, F., S.L. Halgedahl, and D.J. Dunlop, Temperature dependence of magnetic domains in magnetite crystals, *Geophys. Res. Lett., 15,* 499-502, 1988.

Metcalf, M., and M. Fuller, Domain observations of titanomagnetites during hysteresis at elevated temperatures and thermal cycling, *Phys. Earth Planet. Inter., 46,* 120-126, 1987.

Néel, L., Théorie du traînage magnétique des ferromagnétiques en grains fins avec applications aux terres cuites, *Ann. Géophys., 5,* 99-136, 1949.

Néel, L., Some theoretical aspects of rock magnetism, *Adv. Phys., 4,* 191-242, 1955.

Özdemir, Ö., and W. O'Reilly, An experimental study of the intensity and stability of thermoremanent magnetization acquired by synthetic monodomain titanomagnetite substituted by aluminium, *Geophys. J. R. Astron. Soc., 70,* 141-154, 1982.

Parry, L.G., Magnetization of multidomain particles of magnetite, *Phys. Earth Planet. Inter., 19,* 21-30, 1979.

Pauthenet, R., and L. Bochirol, Aimantation spontanée des ferrites, *J. Phys. Radium, 12,* 249-251, 1951.

Schmidt, V.A., A multidomain model of thermoremanence, *Earth Planet. Sci. Lett., 20,* 440-446, 1973.

Schmidt, V.A., The variation of the blocking temperature in models of thermoremanence (TRM), *Earth Planet. Sci. Lett., 29,* 146-154, 1976.

Shcherbakov, V.P., E. McClelland, and V.V. Shcherbakova, A model of multidomain thermoremanent magnetization incorporating temperature-variable domain structure, *J. Geophys. Res., 98,* 6201-6216, 1993.

Stacey, F.D., Thermo-remanent magnetization (TRM) of multidomain grains in igneous rocks, *Philos. Mag., 3,* 1391-1401, 1958.

Stacey, F.D., The physical theory of rock magnetism, *Adv. Phys., 12,* 45-133, 1963.

Street, R., and J.C. Woolley, A study of magnetic viscosity, *Proc. Phys. Soc., A62,* 562-572, 1949.

Thellier, E., Sur l'aimantation des terres cuites et ses application géophysiques, *Ann. Inst. Phys. Globe Univ. Paris, 16,* 157-302, 1938.

Tucker, P., and W. O'Reilly, The acquisition of thermoremanent magnetization by multidomain single crystal titanomagnetite, *Geophys. J. R. Astron. Soc., 60,* 21-36, 1980.

Worm, H-U., M. Jackson, P. Kelso, and S.K. Banerjee, Thermal demagnetization of partial thermoremanent magnetization, *J. Geophys. Res., 93,* 12,196-12,204, 1988.

Xu, S., and D.J. Dunlop, Theory of partial thermoremanent magnetization in multidomain grains, 2, Effect of microcoercivity distribution and comparison with experiment, *J. Geophys. Res., 99,* this issue.

Xu, S., and R.T. Merrill, Microstress and microcoercivity in multidomain grains, *J. Geophys. Res., 94,* 10,627-10,636, 1989.

D. J. Dunlop and S. Xu, Geophysics Laboratory, Department of Physics, University of Toronto, Erindale Campus, Mississauga, Ontario, Canada L5L 1C6.

(Received December 10, 1992;
revised August 30, 1993;
accepted September 8, 1993.)